Supplementary Material

1 Supplementary text S1 - Tremor detection

For the identification of tremors, we use an approach of automatic seismic event detection proposed by Roman (2017), that has been successfully implemented in Ramakrushana Reddy et al. (2020). This method works on individual channel of data (we utilized vertical channel of seismometer).It takes advantage of the fact that harmonic tremor resembles speech and music (it contains signal of the fundamental frequency and arbitrary number of harmonics of this signal present in the spectrum).

We initially assume that all data contains tremor. The detection process is independently done on small subset of the signal (1 minute in our case). In the first step, Harmonic Product Spectrum (HPS) (Noll, 1969) is used for determination of the fundamental frequency of a signal. It is a result of arbitrary (5 in our case) successive decimations of the fast Fourier transform of the signal and is given by (Roman, 2017):

$$Y(\omega) = \prod_{r=1}^{5} |X(\omega r)| \qquad \text{S1}$$

Y(ω) is HPS, X(ω) is a minute of continuous seismological data.

The fundamental frequency F_0 is the one with the maximum power value of the resulting HPS.
The arbitrary N number of harmonic frequencies is then obtained by the integer multiplication of F_0 (2,3,4…). In our case N=1, so just a fundamental frequency with one harmonic fit this criterion (for example for F_0 = 2Hz, first harmonic at 4Hz).

For each fundamental and harmonic frequency, we define the interharmonic (IH) frequency as the frequency with the maximum value of power X(ω) in the middle part (between the first and third quartiles) of the interharmonic frequency interval.

The measure of tremor presence in the minute of data is then estimated using Harmonic Strength Index (HSI), calculated for each fundamental frequency – harmonic pair and given by:

$$HSI_i = \frac{X(F_i)}{X(IH_i)} \qquad \text{S2}$$

HSI_i is the Harmonic Strength Index for i=1,2,3… harmonic frequency, $X(F_i)$ is the power of the signal at a fundamental or harmonic and $X(IH_i)$ is the power at its interharmonic.

The larger value of HSI indicates stronger presence of a tremor. We computed HIS, fundamental frequency and its harmonic separately for each minute of data and opted for following criteria to detect the presence of tremor in data, following Roman (2017):

- F_0 must be between 1 and 6 Hz

- One harmonic must be present
- HSI for this harmonic must be 2.0 or higher
- Continuous tremor detection for at least two minutes (reject single window detections)

We summed up all the durations of tremor occurrences in hour-long intervals and represent results as tremor time-fraction for every hour. We then calculated basic statistics about the daily presence of harmonic tremor in vertical channel of each OBS.

2 Supplementary text S2 – Tremor analysis

The median daily duration of harmonic tremor for OBS-1 is 17.05 h (with 15.56-18.95 25th percentile range), OBS-4 is 4.76 h (with 2.75-7.76 25th percentile range), and OBS-5 is 10.14 h (with 6.29-12.72 25th percentile range). The presence of the harmonic tremor was most consistent for OBS-1, as the variance of the tremor length in OBS-1 (6.00 h) is lower compared to OBS-4 (19.23 h) and OBS-5 (15.09 h).

By looking at the seismograms manually, we observe in general that tremor presence on a daily basis usually resemble the cycles observed for ocean tides, i.e., division of each day into four, roughly 6 h long cycles of alternating observed tremor states. Within each period of tremor presence, except small (few minutes) breaks, we observe them continuously.

Periodogram plots of tremor time-fraction also show distinct peaks around 12.4 h in OBS-1 and OBS-4 (M2 in Figure S1), and peaks corresponding to M4 and MS4 (shallow water quarter diurnal constituent) in OBS-4 (Figure S1). There is an additional peak for OBS-1 at 23.91 h (K1 in Figure S1) and a small peak at OBS-4 (K2 in Figure S1). We attribute these two peaks to lunar diurnal (K1) and lunisolar semi-diurnal (K2) constituents. None of these components are present on the tremor periodogram of OBS-5. Periodicities of individual tidal components are listed in Table S1.

Wide peaks around 705-710 h visible on all three periodograms are probably caused by synodic periodicity of the Moon position relative to the Sun and the Earth (2 x 14 days x 24 h - Ms), and the highest period peaks for OBS-1 and OBS-4 can be the first overtone of the semiannual solar period of tides (0.5 x 182.6 days x 24 h = 2191.2 h).

Notably, the local maxima for roughly 66.7, 119.5 and 288 h are repeated on tremor periodograms for OBS-1 and OBS-4.

3 Supplementary Figures and Tables

3.1 Supplementary Figures

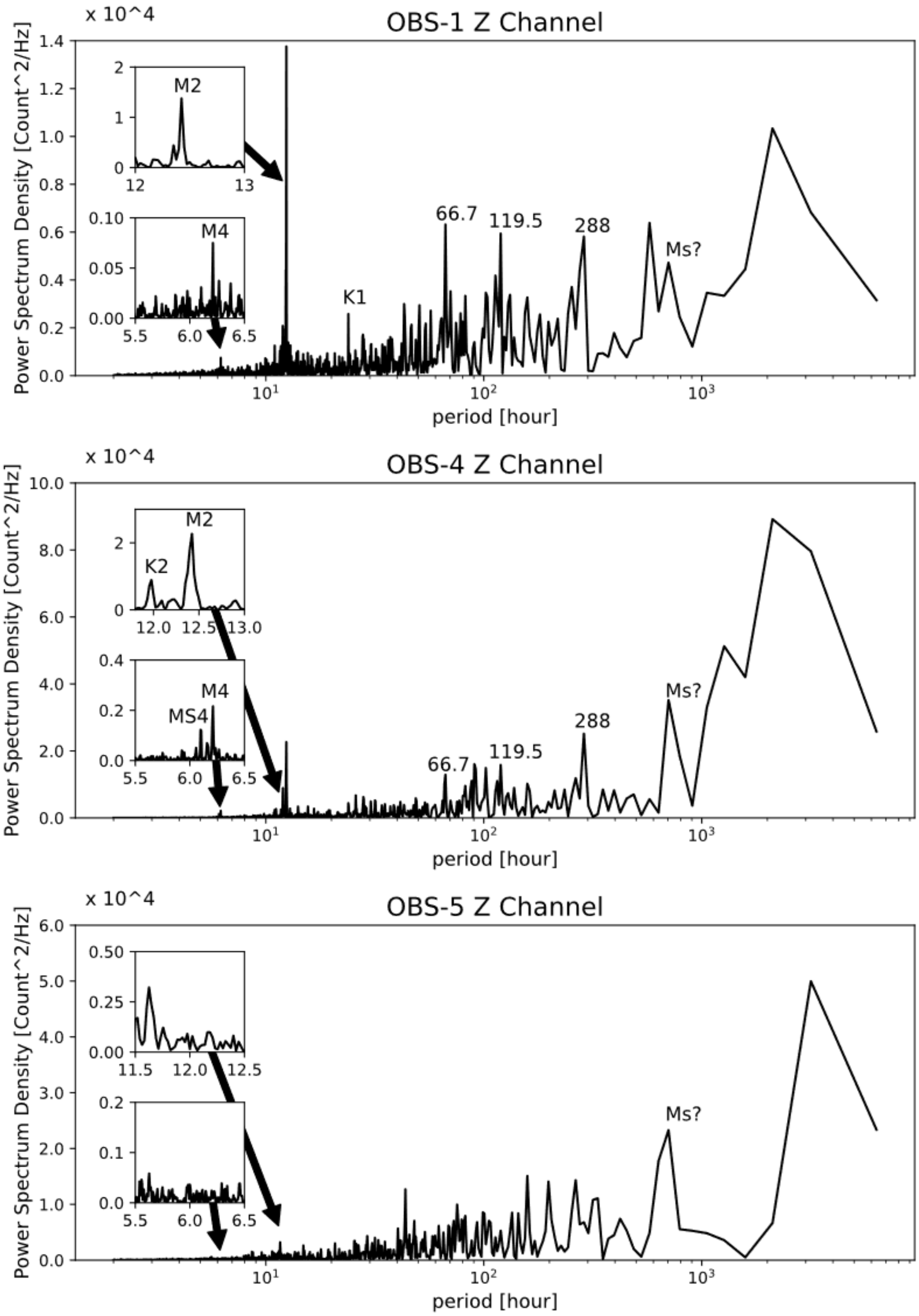

Supplementary Figure S1. Power spectrum density (periodogram) functions for hourly count of tremor on OBS-1, OBS-4, and OBS-5. Annotated picks correspond to tidal constituents: M2 – principal lunar semidiurnal, M4 – shallow water overtides of principal lunar semidiurnal (first overtide of principal lunar semidiurnal), K1 – luni-solar declinational diurnal, Ms? – potential influence of lunar synodic periodicity (2 x 14 days x 24 h), K2 - combined declinational lunar and declinational solar tidal component, MS4. – compound component of M2 and principal solar semidiurnal constituent (S2). Notice that peaks marked with 66.7 h, 119.5 h and 288 h coincide on both OBS-1 and OBS-4.

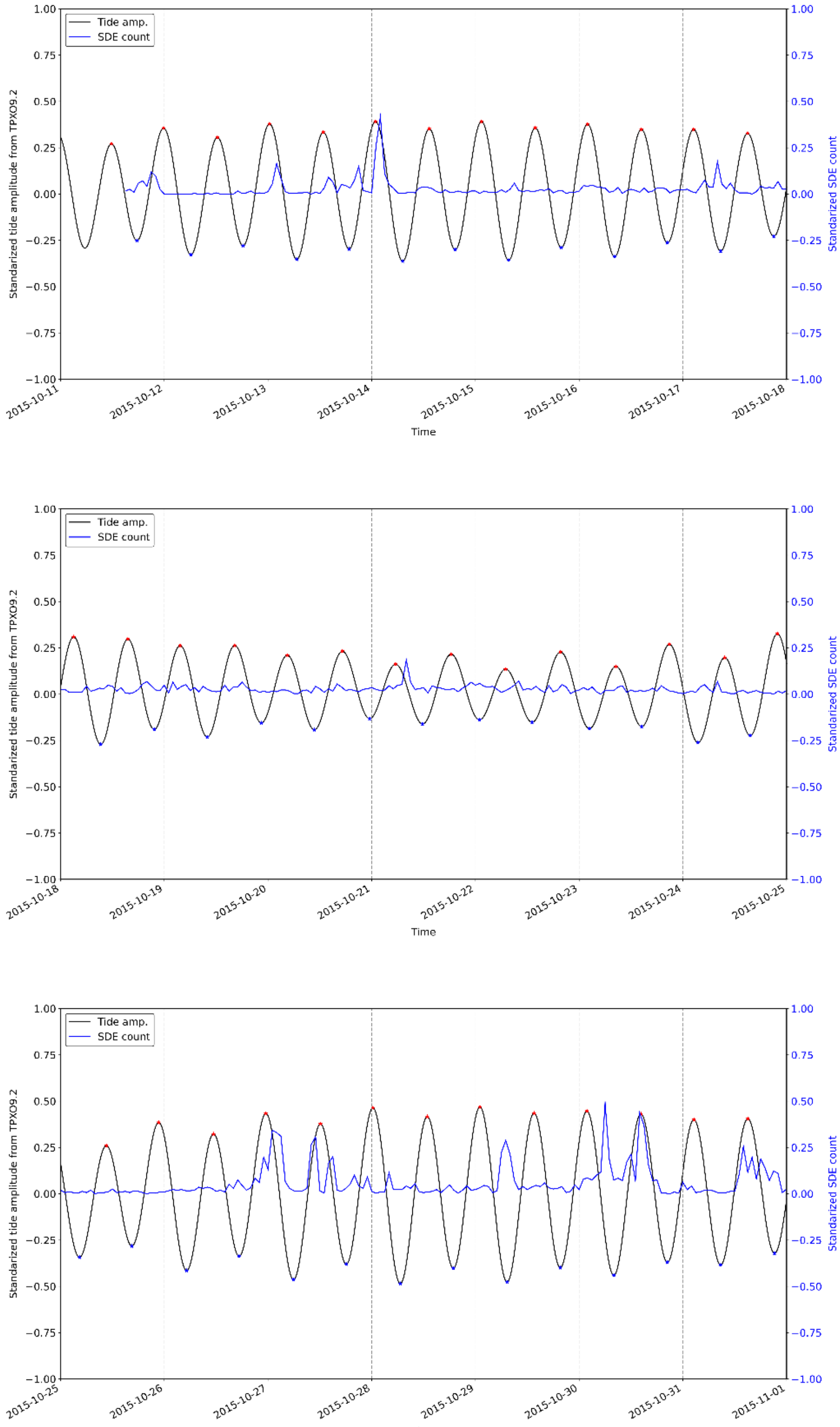

Supplementary Figure S2. Standardized plots of mean sea level amplitude change due to tides (black line) superimposed on short duration events hourly count on OBS-1 (blue line) for weeks 1-3 of survey (11.10-1.11.2015).

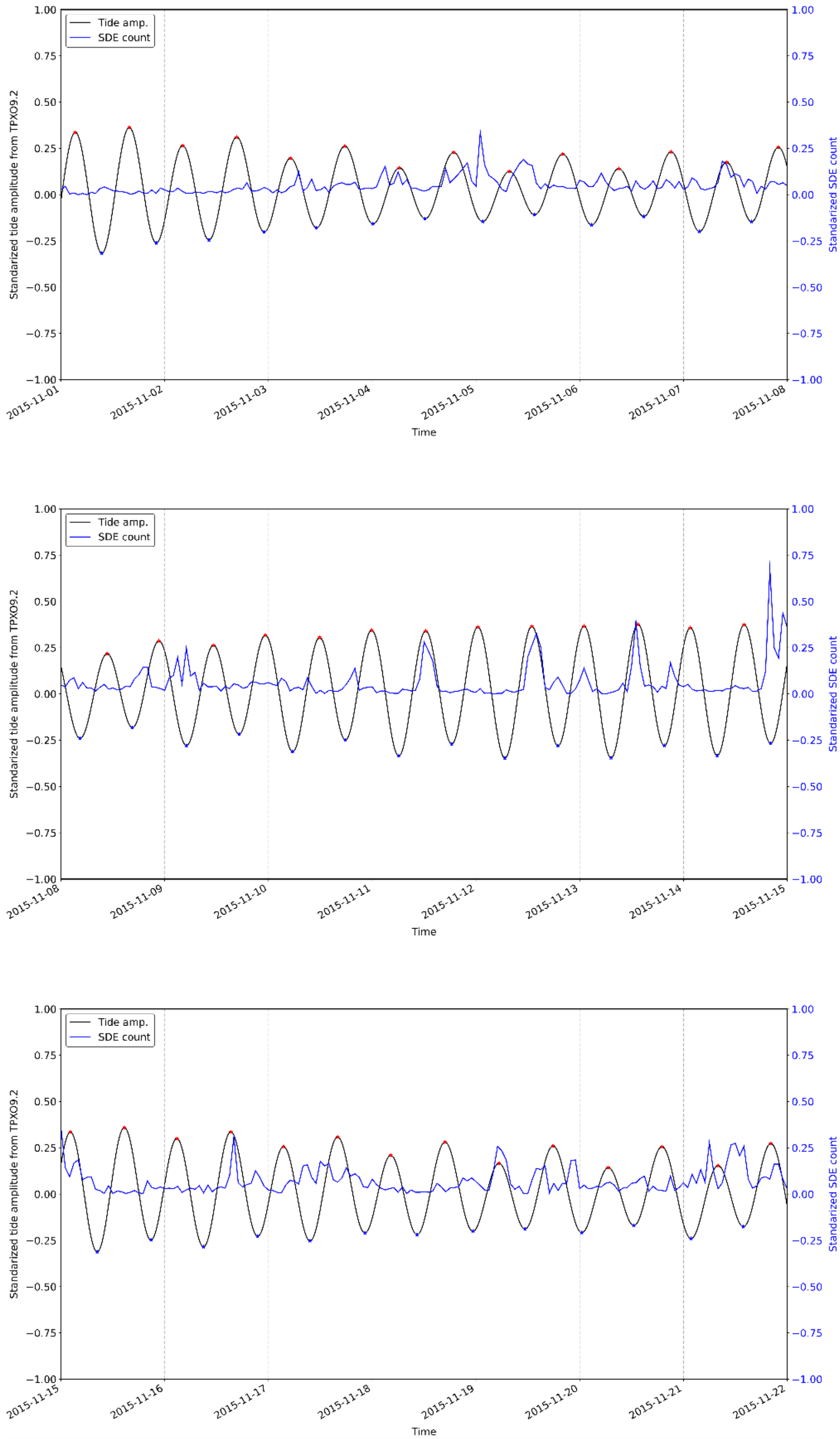

Supplementary Figure S3. Standardized plots of mean sea level amplitude change due to tides (black line) superimposed on short duration events hourly count on OBS-1 (blue line) for weeks 4-6 of survey (1.11-22.11.2015).

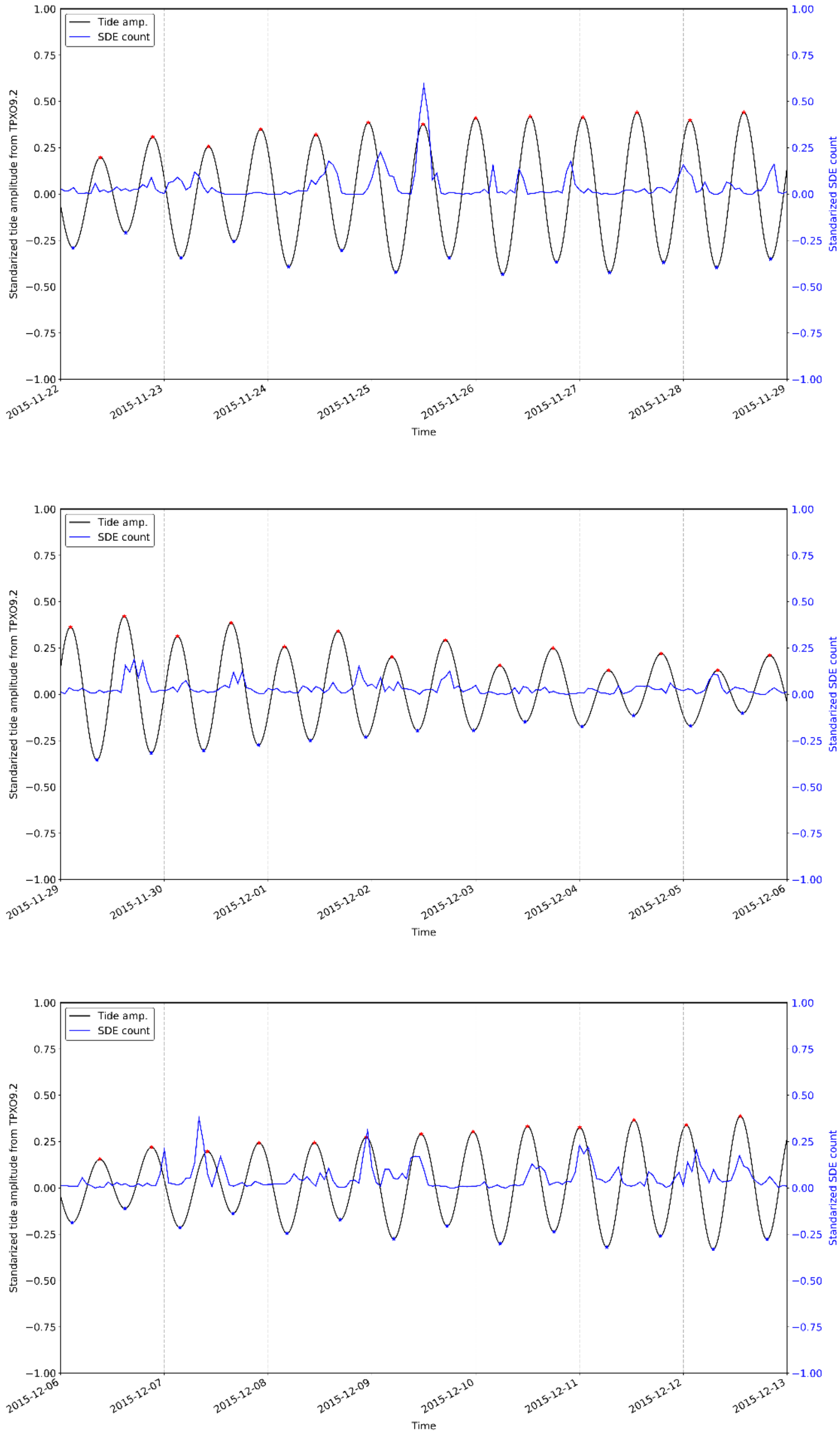

Supplementary Figure S4. Standardized plots of mean sea level amplitude change due to tides (black line) superimposed on short duration events hourly count on OBS-1 (blue line) for weeks 7-9 of survey (22.11-13.12.2015).

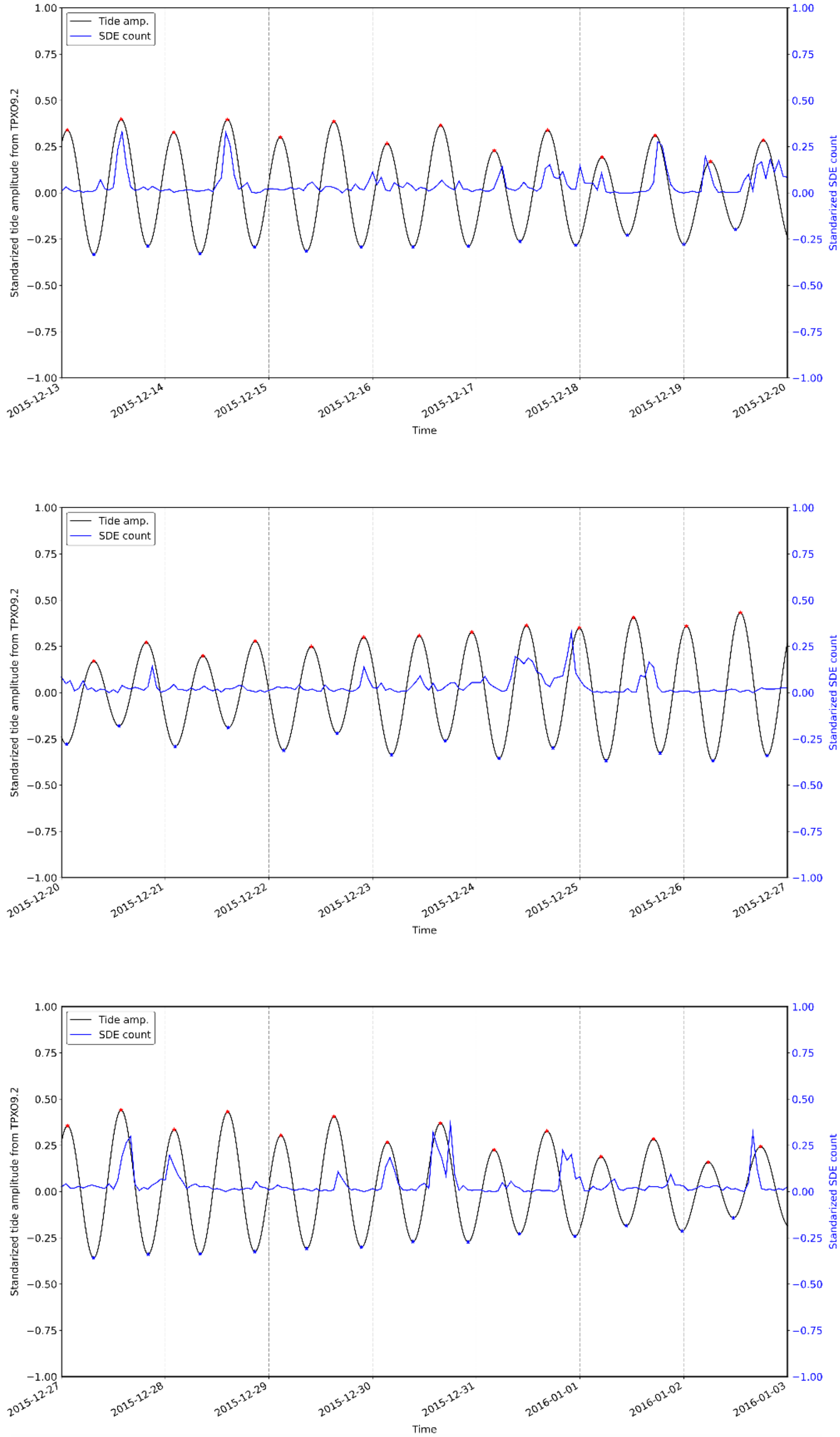

Supplementary Figure S5. Standardized plots of mean sea level amplitude change due to tides (black line) superimposed on short duration events hourly count on OBS-1 (blue line) for weeks 10-12 of survey (13.12.2015-3.1.2016).

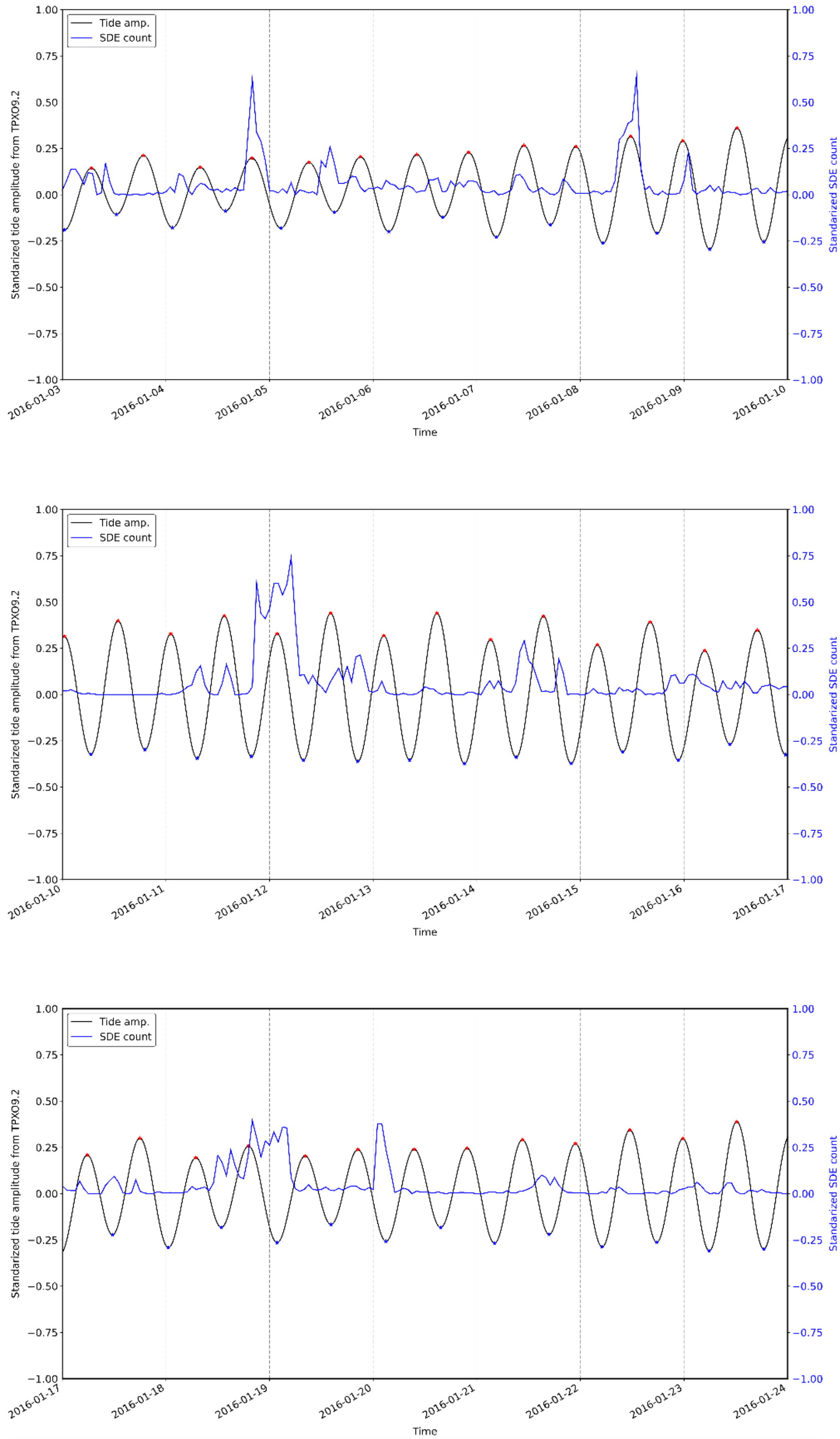

Supplementary Figure S6. Standardized plots of mean sea level amplitude change due to tides (black line) superimposed on short duration events hourly count on OBS-1 (blue line) for weeks 13-15 of survey (3.1-24.1.2016).

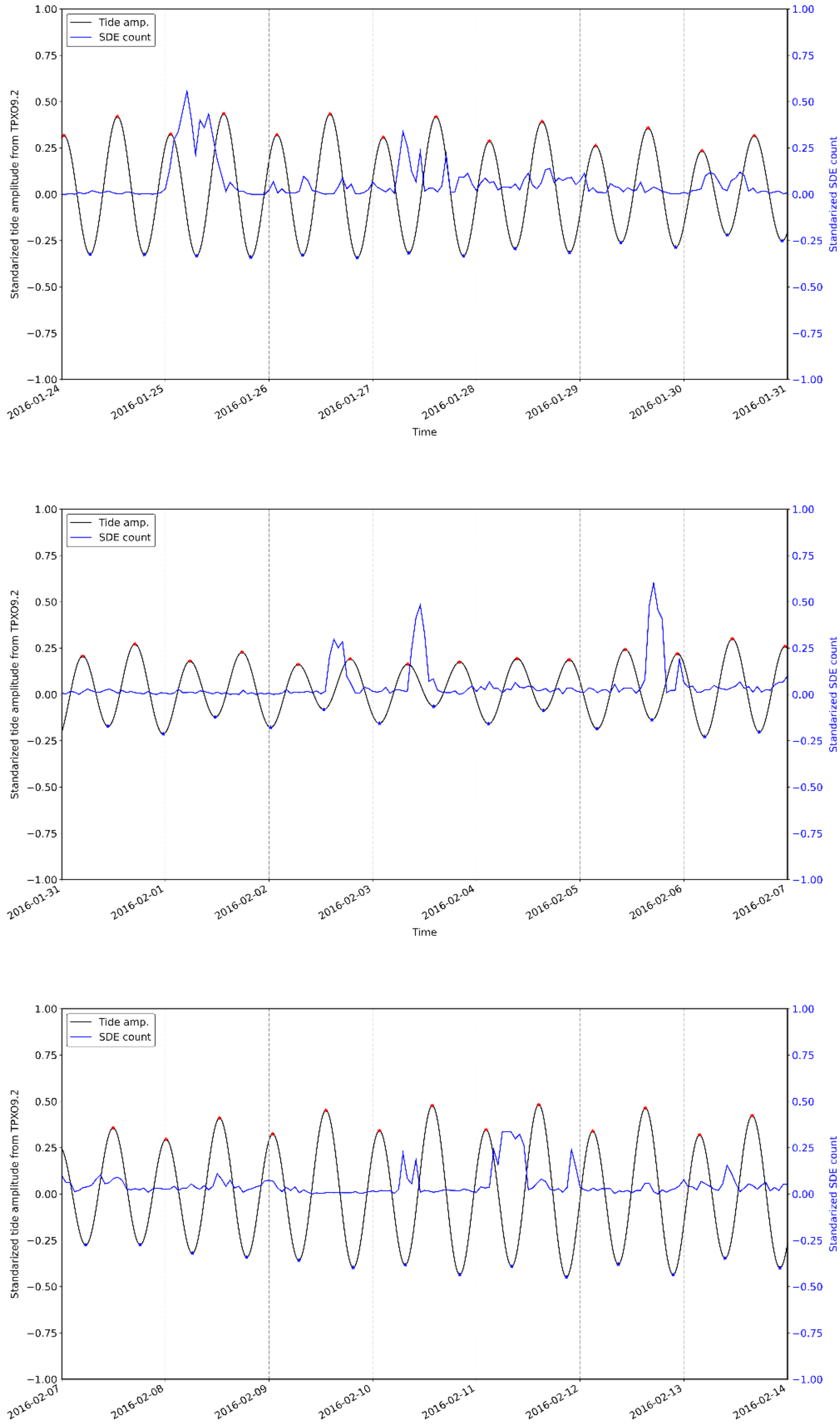

Supplementary Figure S7. Standardized plots of mean sea level amplitude change due to tides (black line) superimposed on short duration events hourly count on OBS-1 (blue line) for weeks 16-18 of survey (24.1-14.2.2016).

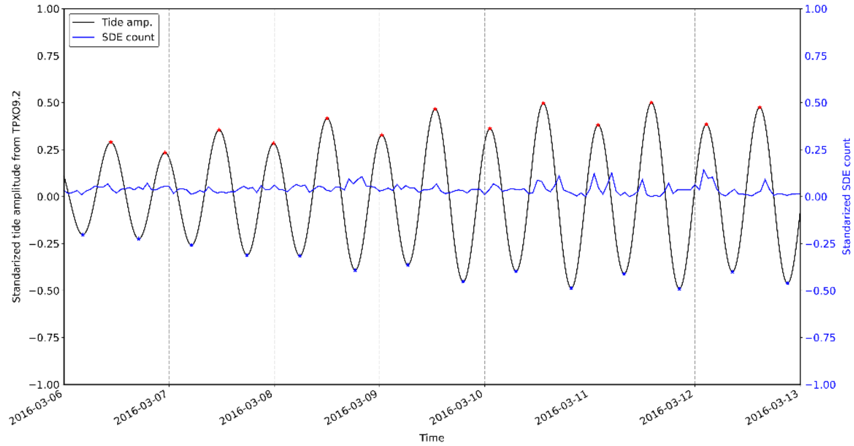

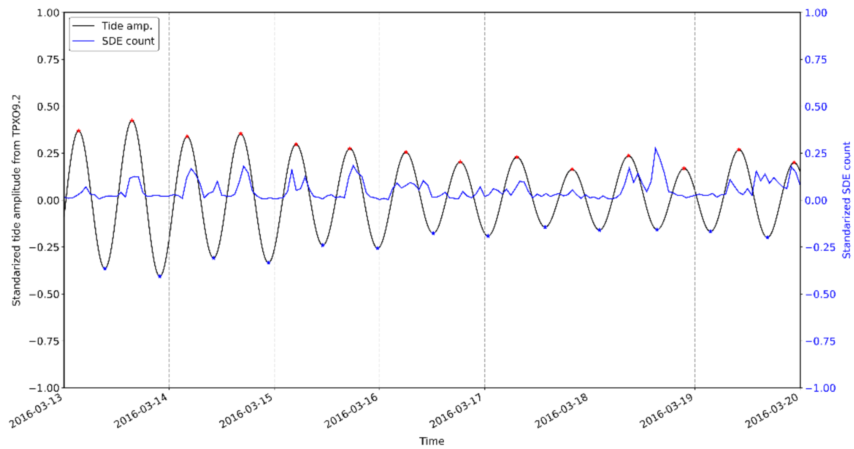

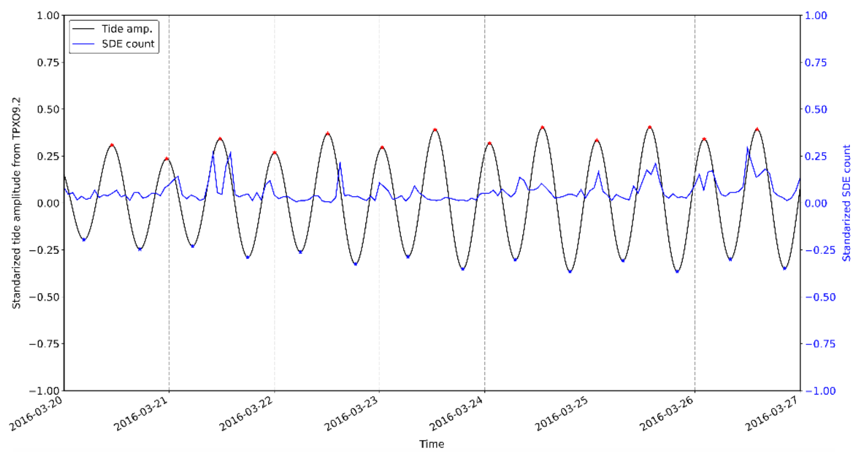

Supplementary Figure S8. Standardized plots of mean sea level amplitude change due to tides (black line) superimposed on short duration events hourly count on OBS-1 (blue line) for weeks 22-24 of survey (6.3-27.3.2016).

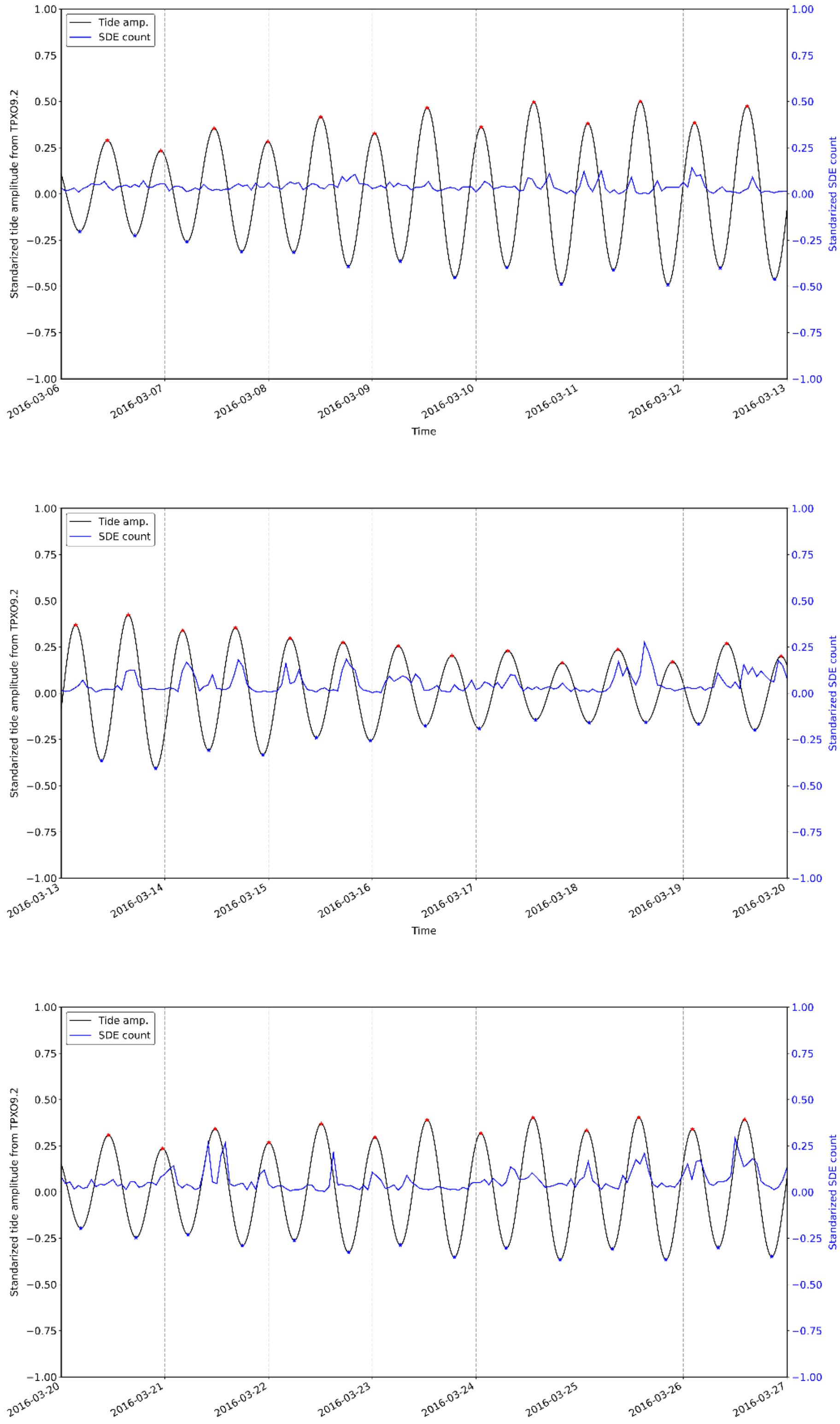

Supplementary Figure S9. Standardized plots of mean sea level amplitude change due to tides (black line) superimposed on short duration events hourly count on OBS-1 (blue line) for weeks 22-24 of survey (6.3-27.3.2016).

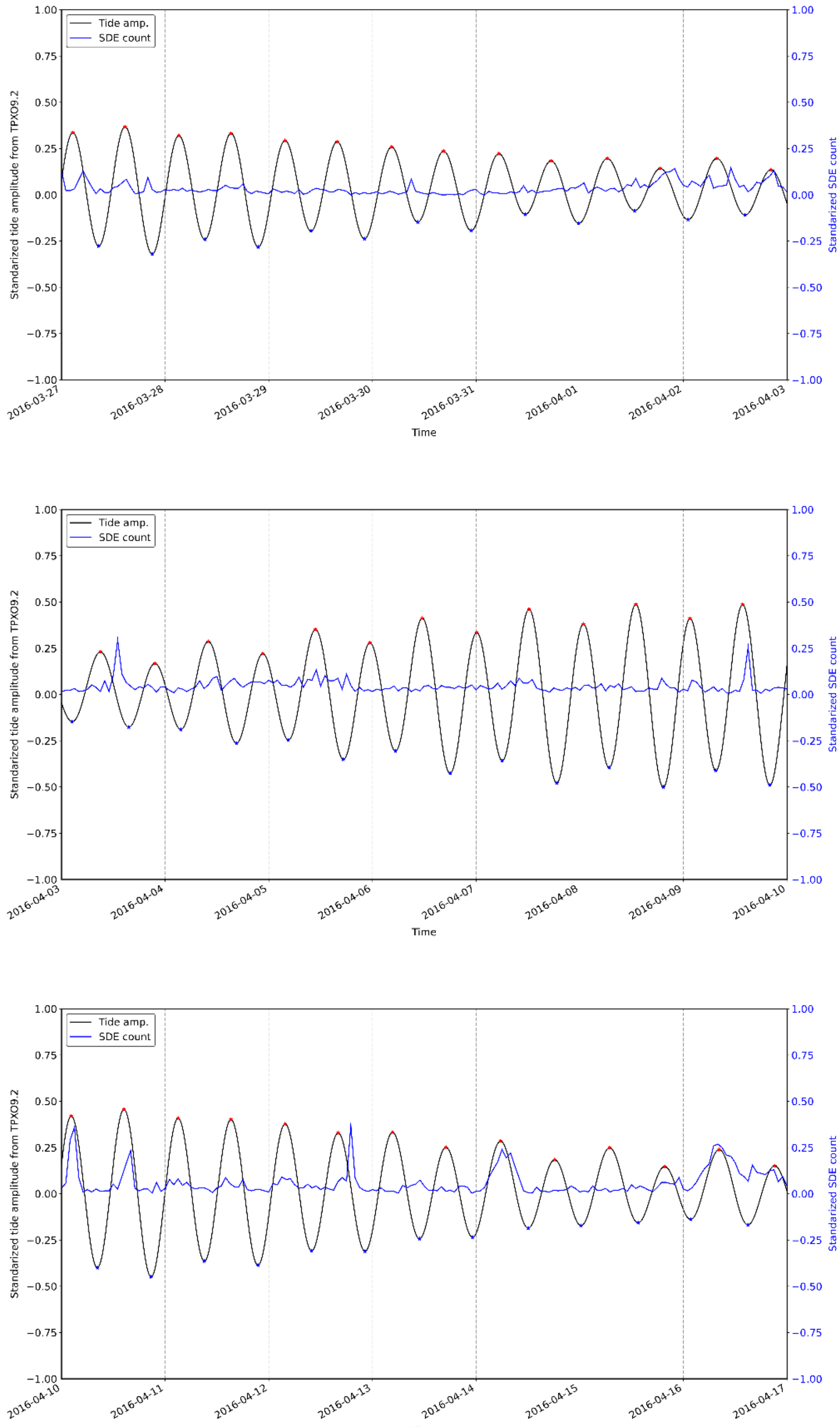

Supplementary Figure S10. Standardized plots of mean sea level amplitude change due to tides (black line) superimposed on short duration events hourly count on OBS-1 (blue line) for weeks 25-27 of survey (27.3-17.4.2016).

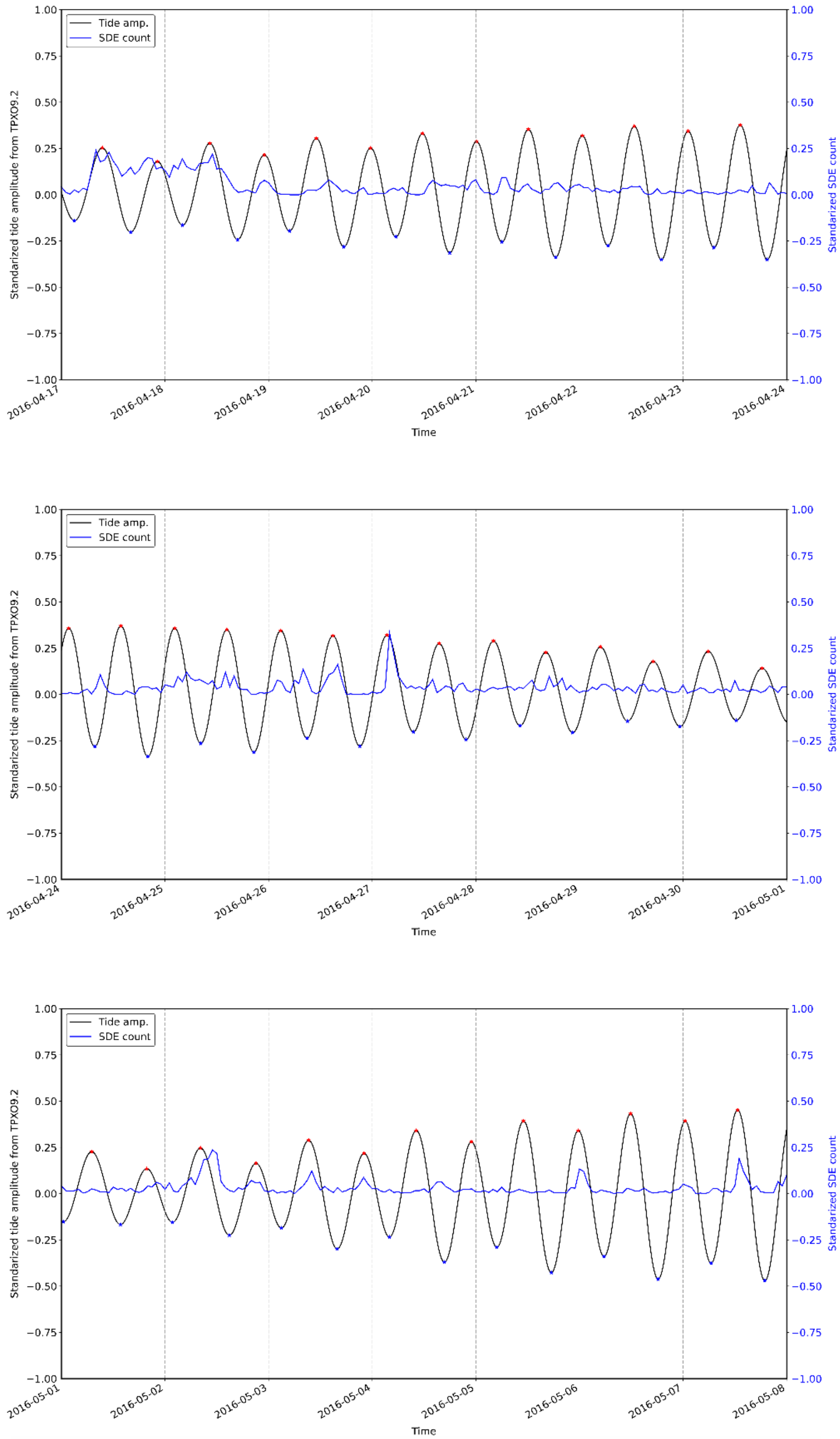

Supplementary Figure S11. Standardized plots of mean sea level amplitude change due to tides (black line) superimposed on short duration events hourly count on OBS-1 (blue line) for weeks 25-27 of survey (17.4-8.5.2016).

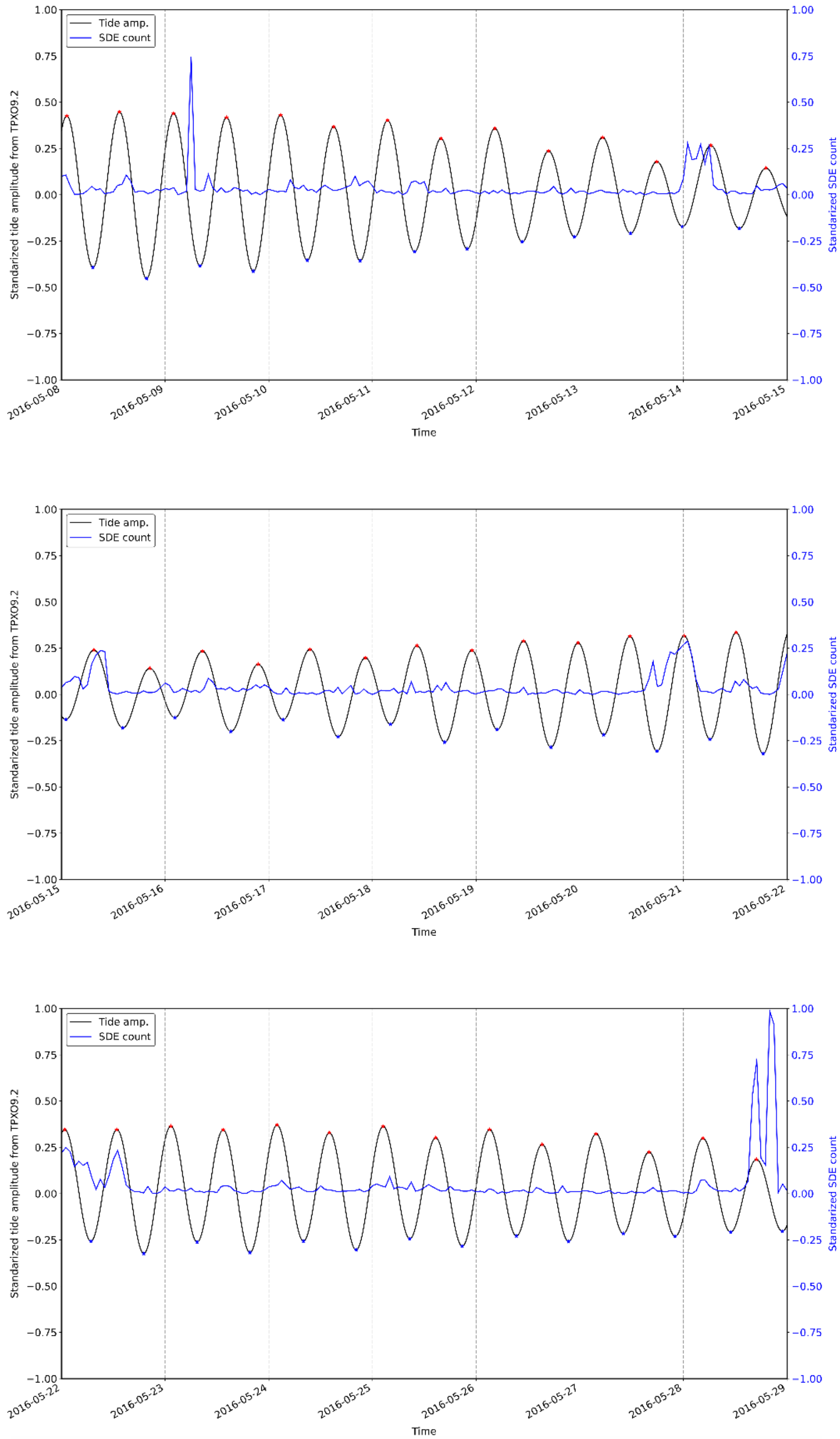

Supplementary Figure S12. Standardized plots of mean sea level amplitude change due to tides (black line) superimposed on short duration events hourly count on OBS-1 (blue line) for weeks 28-30 of survey (8.5-29.5.2016).

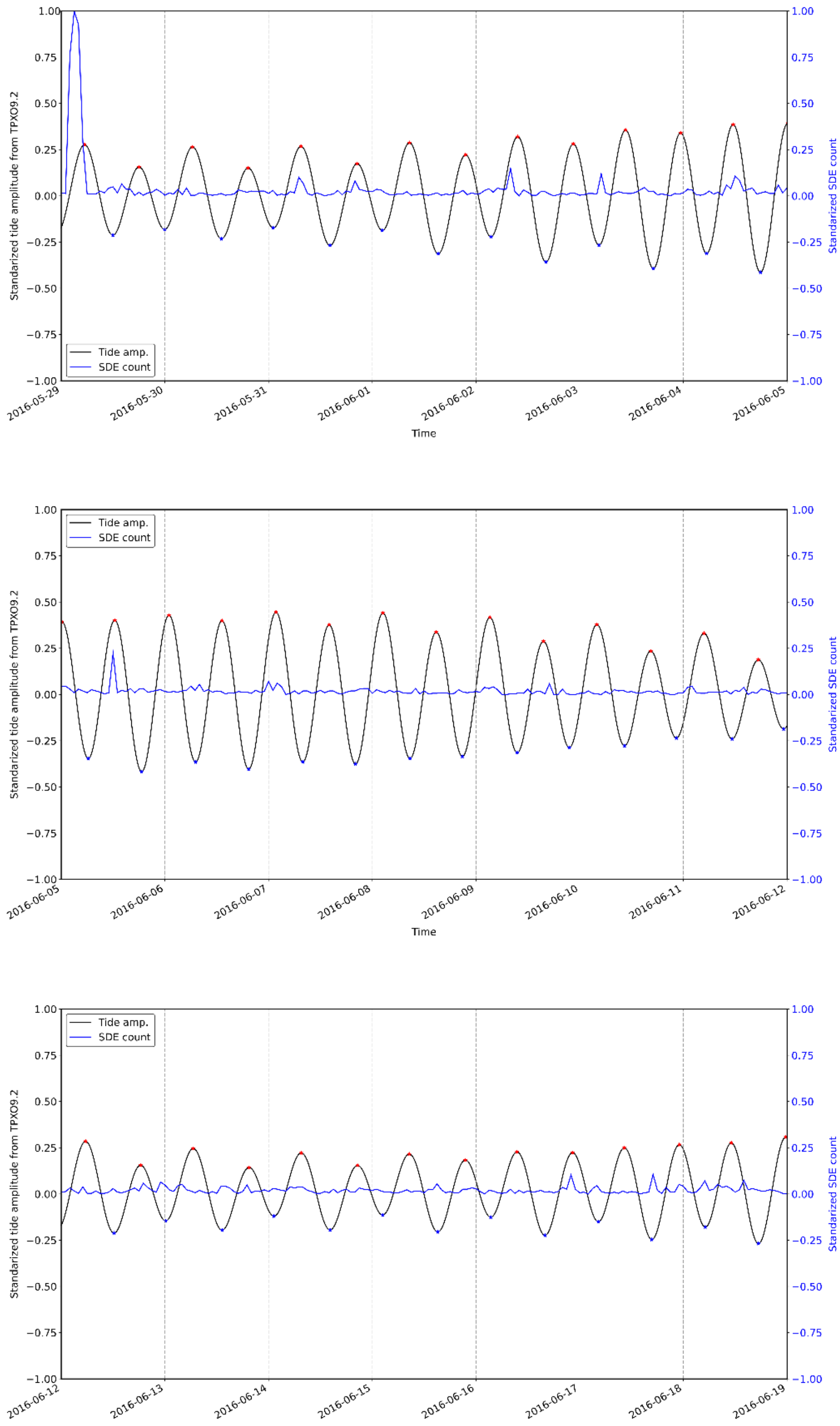

Supplementary Figure S13. Standardized plots of mean sea level amplitude change due to tides (black line) superimposed on short duration events hourly count on OBS-1 (blue line) for weeks 31-33 of survey (29.5-19.6.2016).

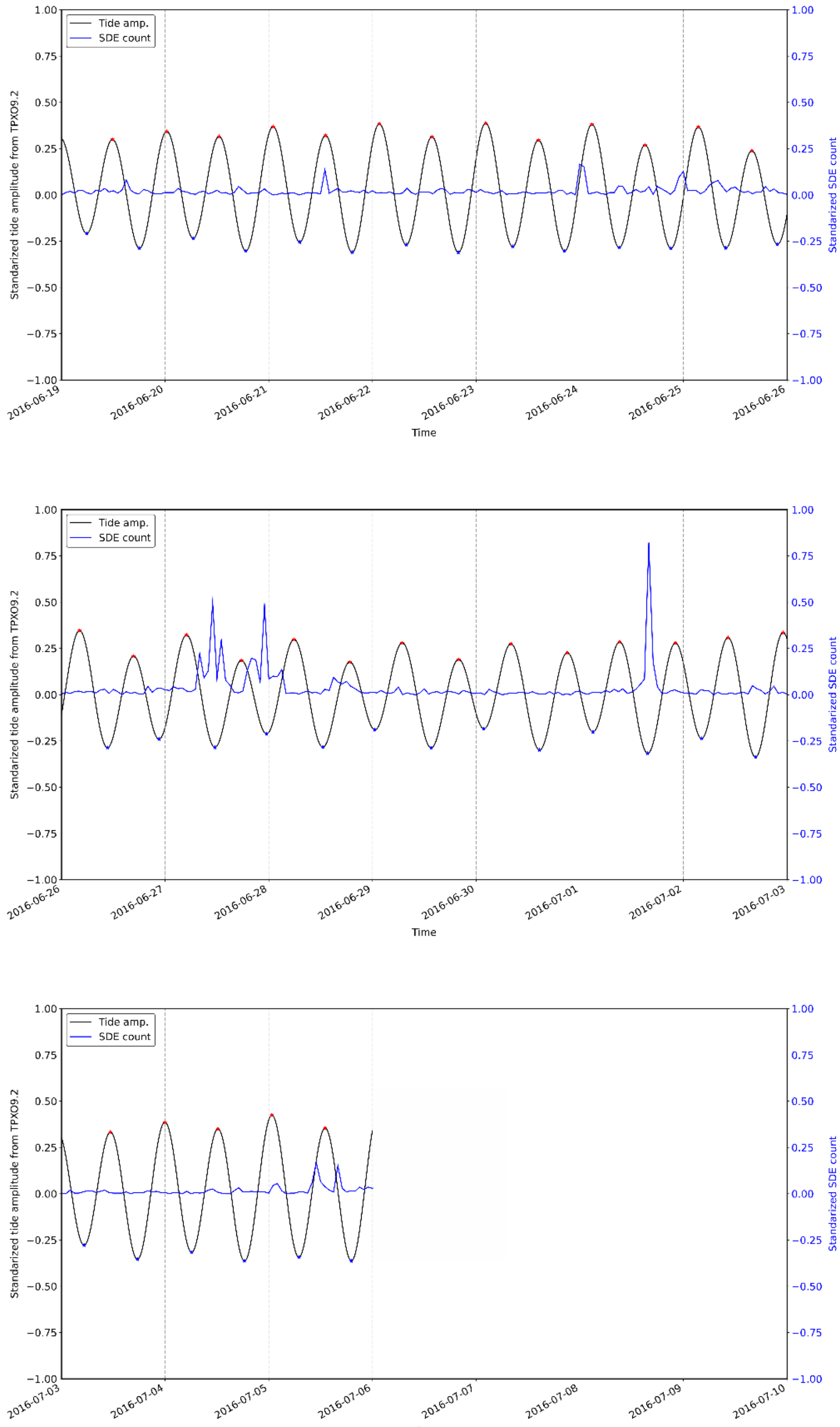

Supplementary Figure S14. Standardized plots of mean sea level amplitude change due to tides (black line) superimposed on short duration events hourly count on OBS-1 (blue line) for weeks 34-36 of survey (19.6-6.7.2016).

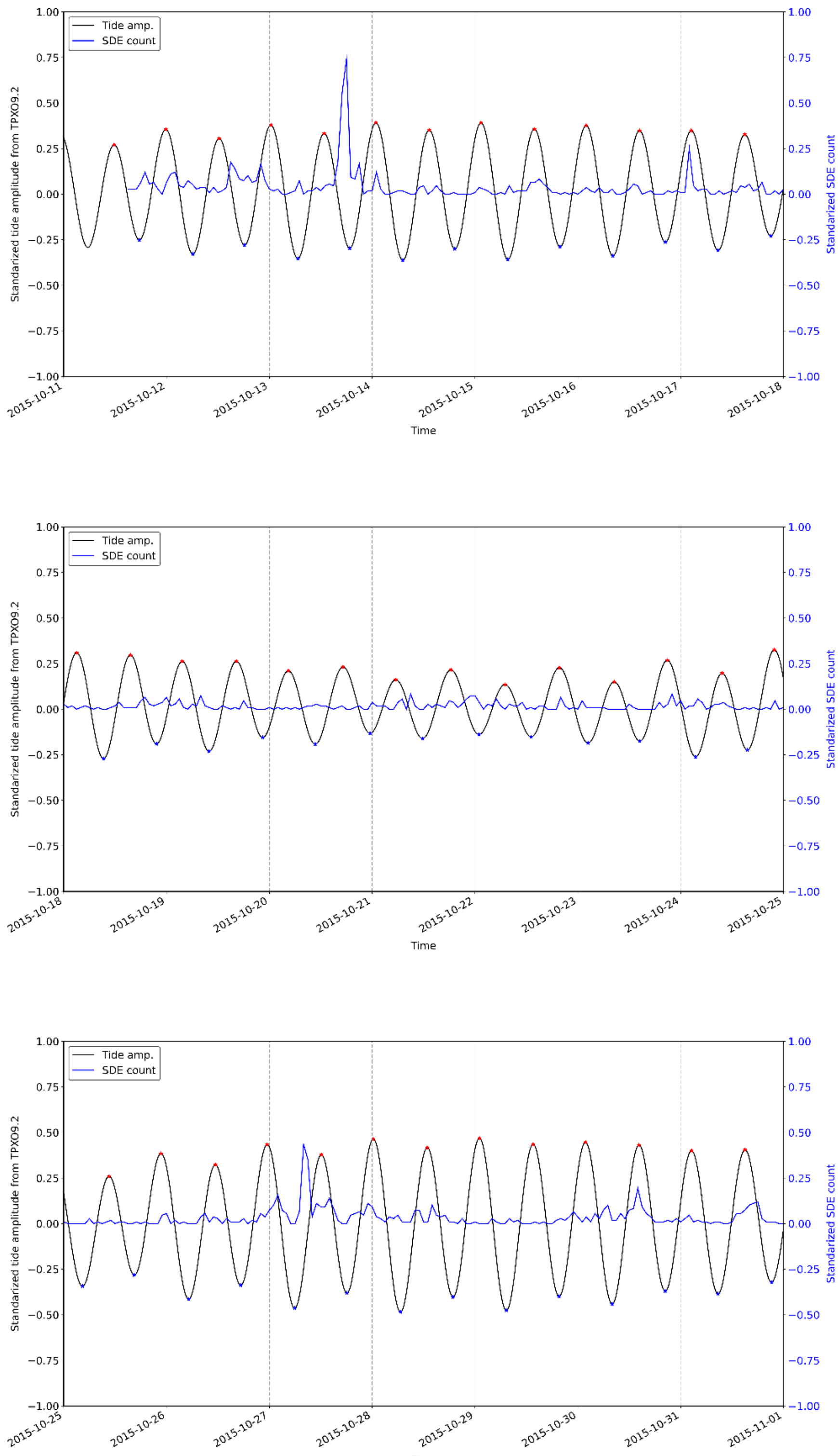

Supplementary Figure S15. Standardized plots of mean sea level amplitude change due to tides (black line) superimposed on short duration events hourly count on OBS-4 (blue line) for weeks 1-3 of survey (11.10-1.11.2015).

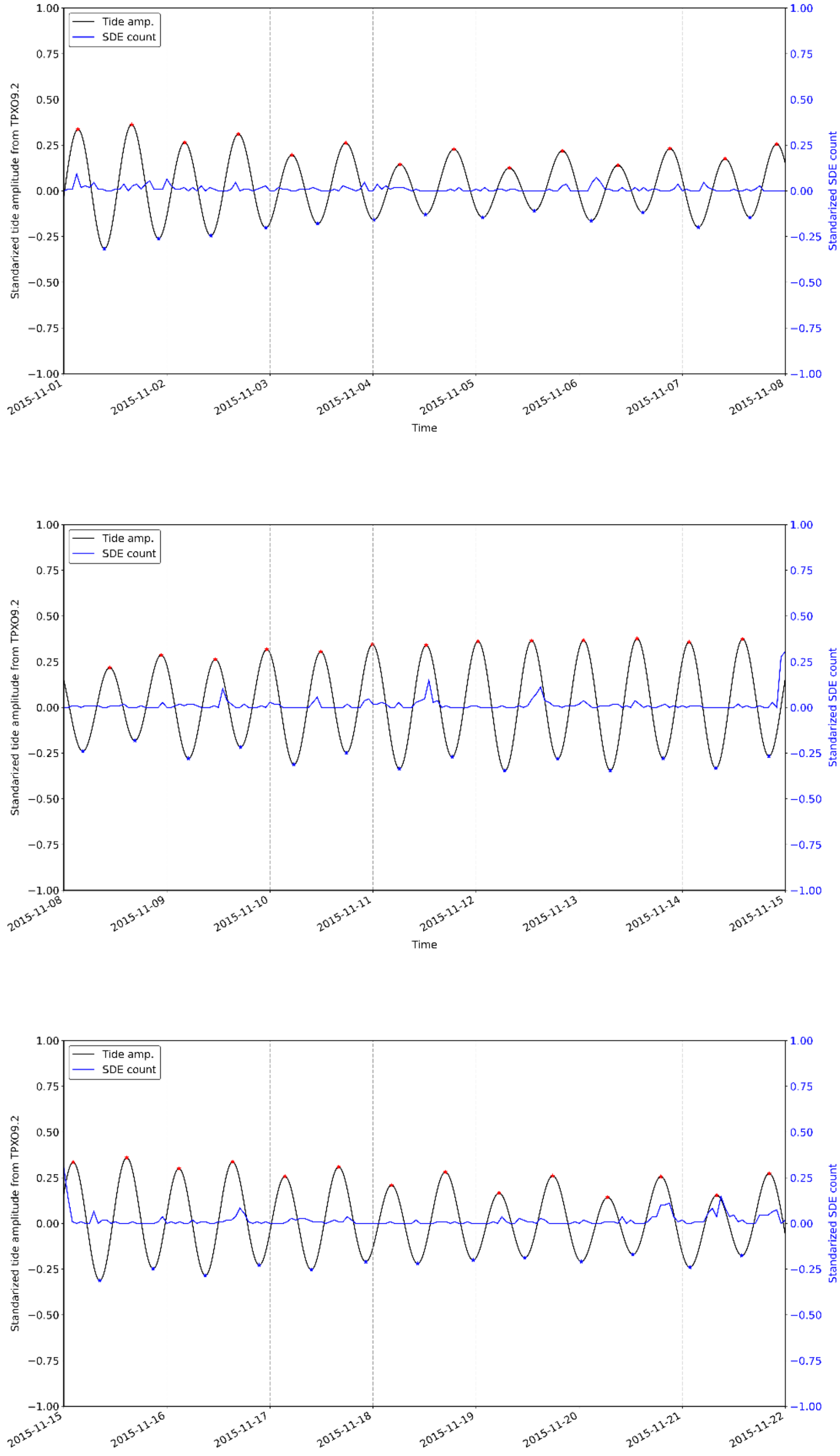

Supplementary Figure S16. Standardized plots of mean sea level amplitude change due to tides (black line) superimposed on short duration events hourly count on OBS-4 (blue line) for weeks 4-6 of survey (1.11-22.11.2015).

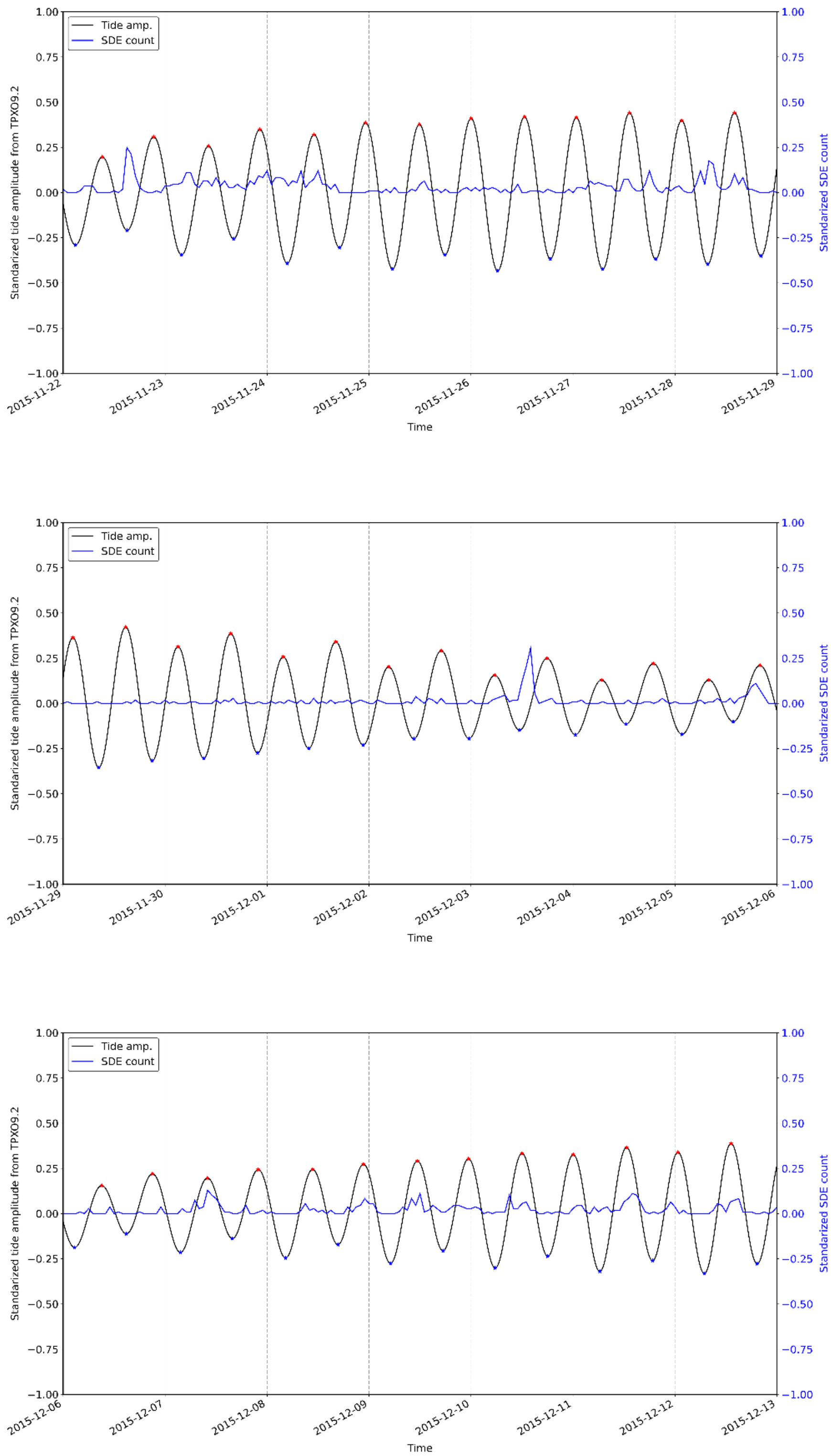

Supplementary Figure S17. Standardized plots of mean sea level amplitude change due to tides (black line) superimposed on short duration events hourly count on OBS-4 (blue line) for weeks 7-9 of survey (22.11-13.12.2015).

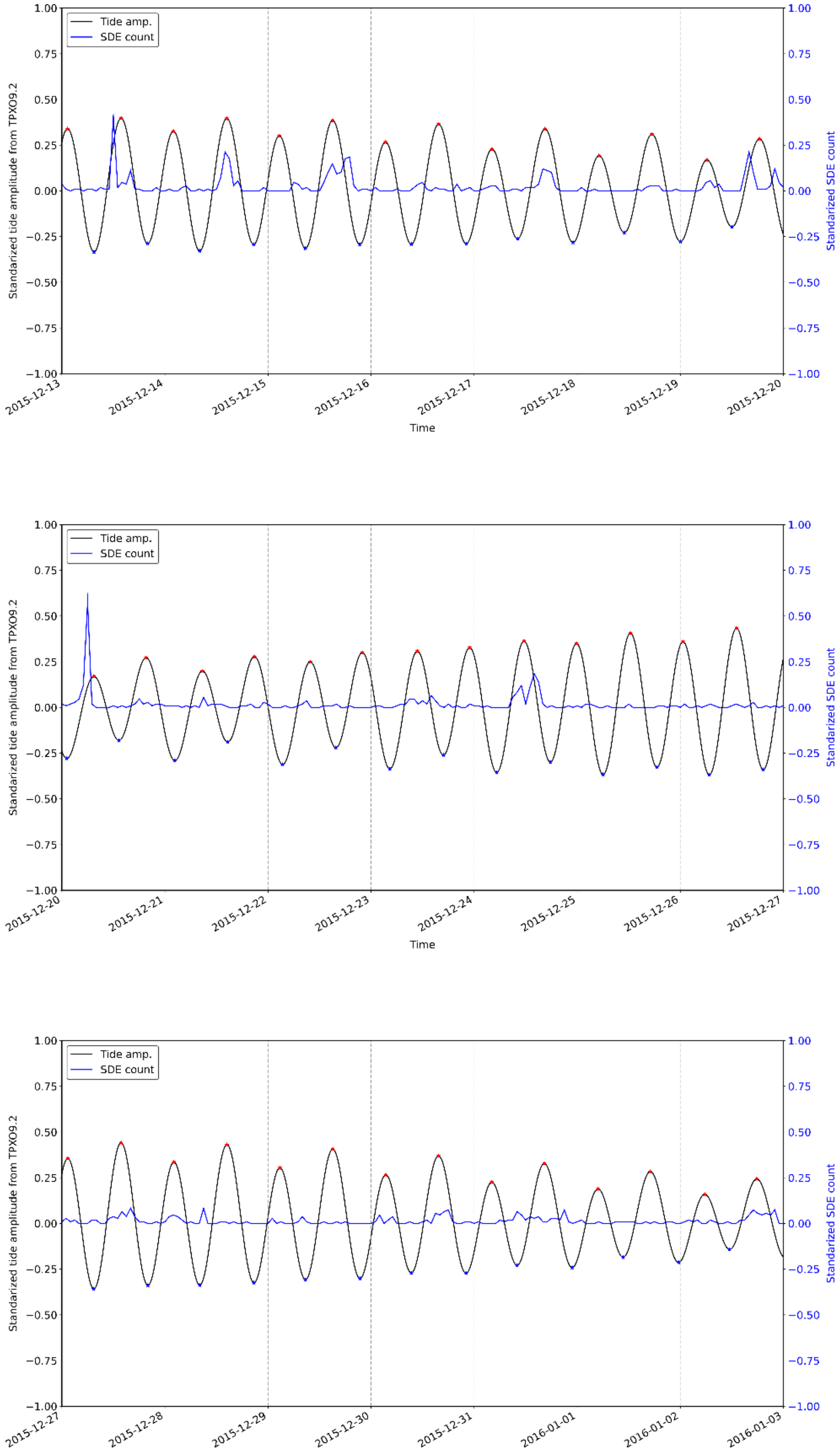

Supplementary Figure S18. Standardized plots of mean sea level amplitude change due to tides (black line) superimposed on short duration events hourly count on OBS-4 (blue line) for weeks 10-12 of survey (13.12.2015-3.1.2016).

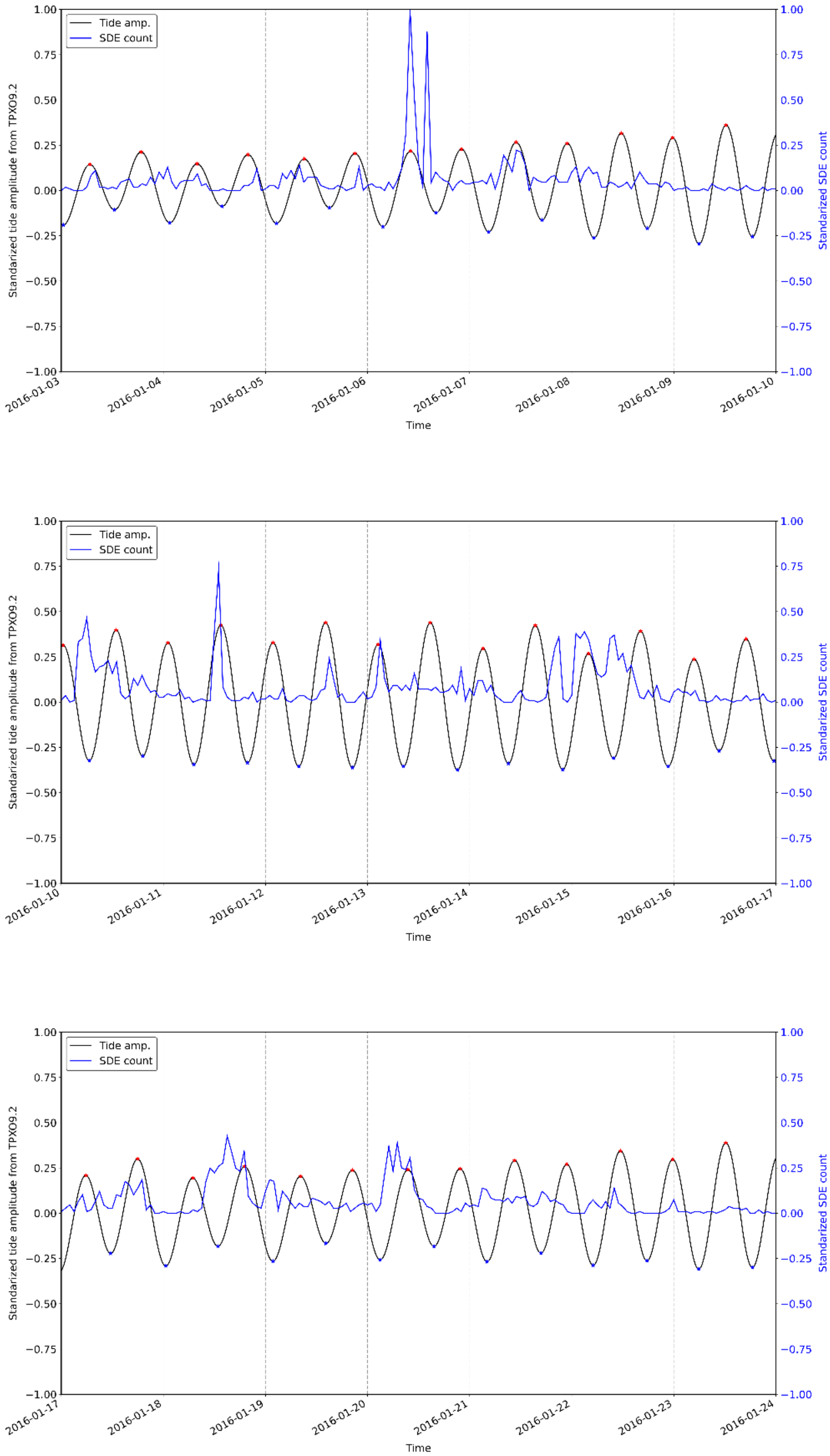

Supplementary Figure S19. Standardized plots of mean sea level amplitude change due to tides (black line) superimposed on short duration events hourly count on OBS-4 (blue line) for weeks 13-15 of survey (3.1-24.1.2016).

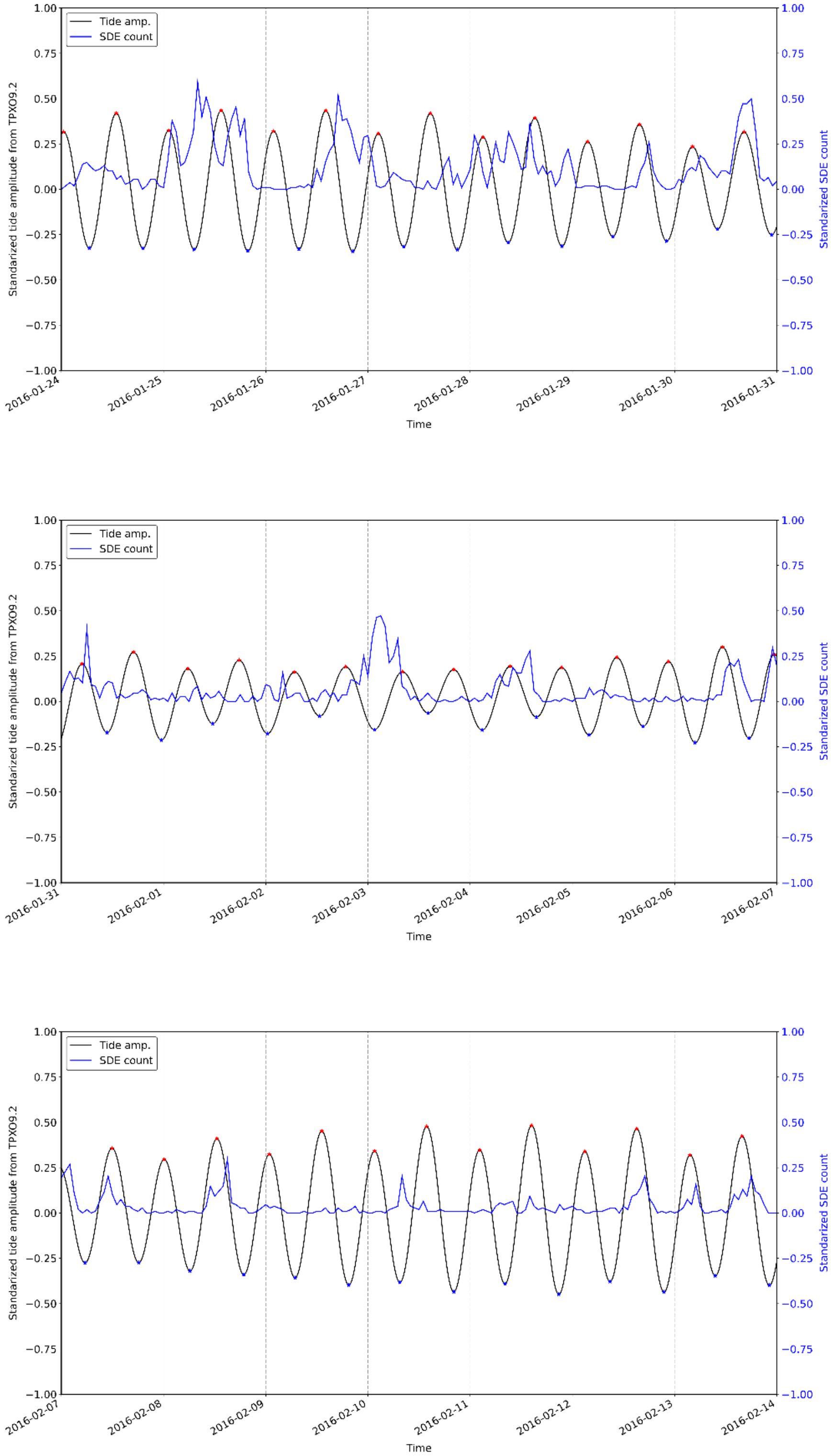

Supplementary Figure S20. Standardized plots of mean sea level amplitude change due to tides (black line) superimposed on short duration events hourly count on OBS-4 (blue line) for weeks 16-18 of survey (24.1-14.2.2016).

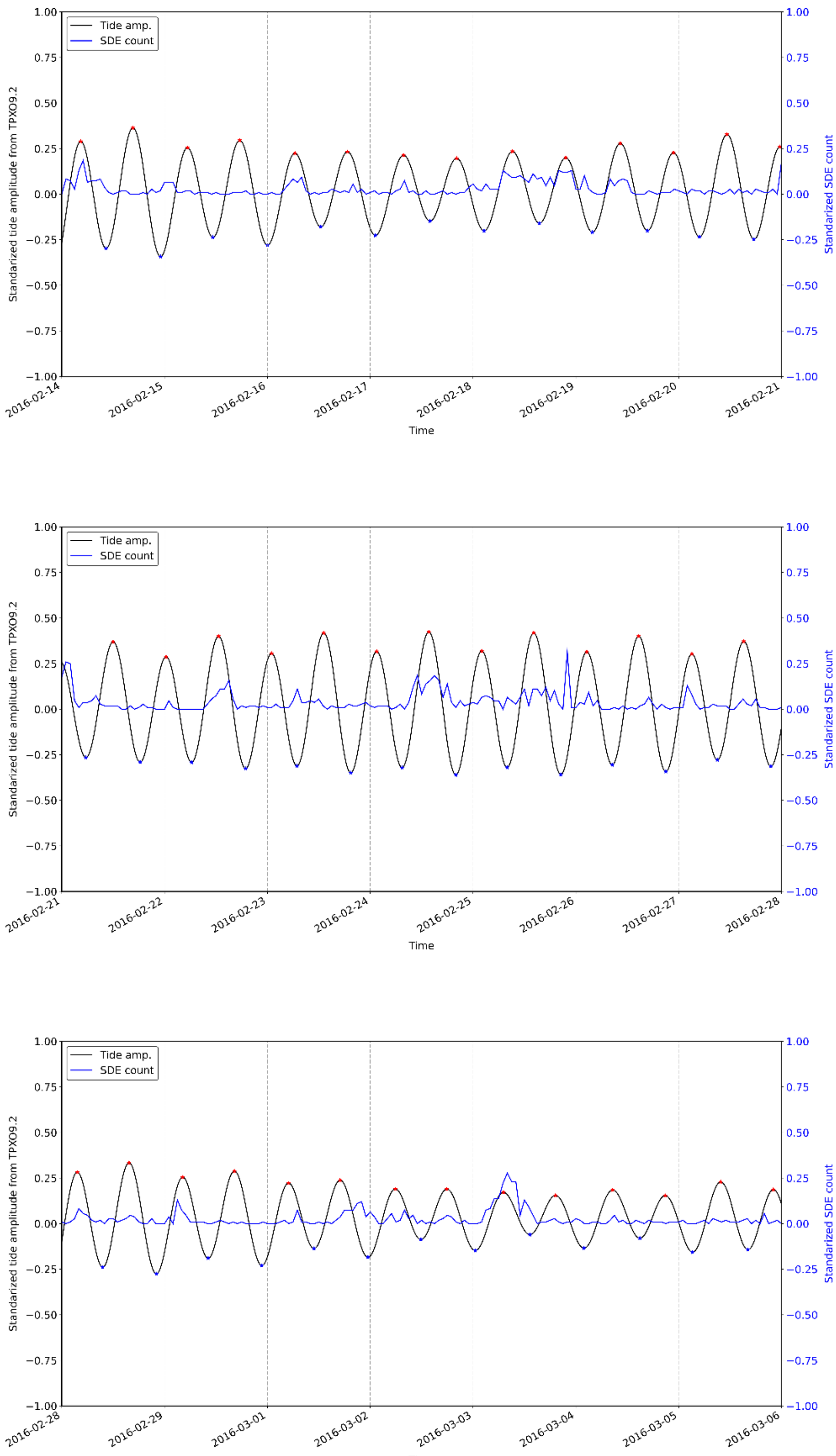

Supplementary Figure S21. Standardized plots of mean sea level amplitude change due to tides (black line) superimposed on short duration events hourly count on OBS-4 (blue line) for weeks 19-21 of survey (14.2-6.3.2016).

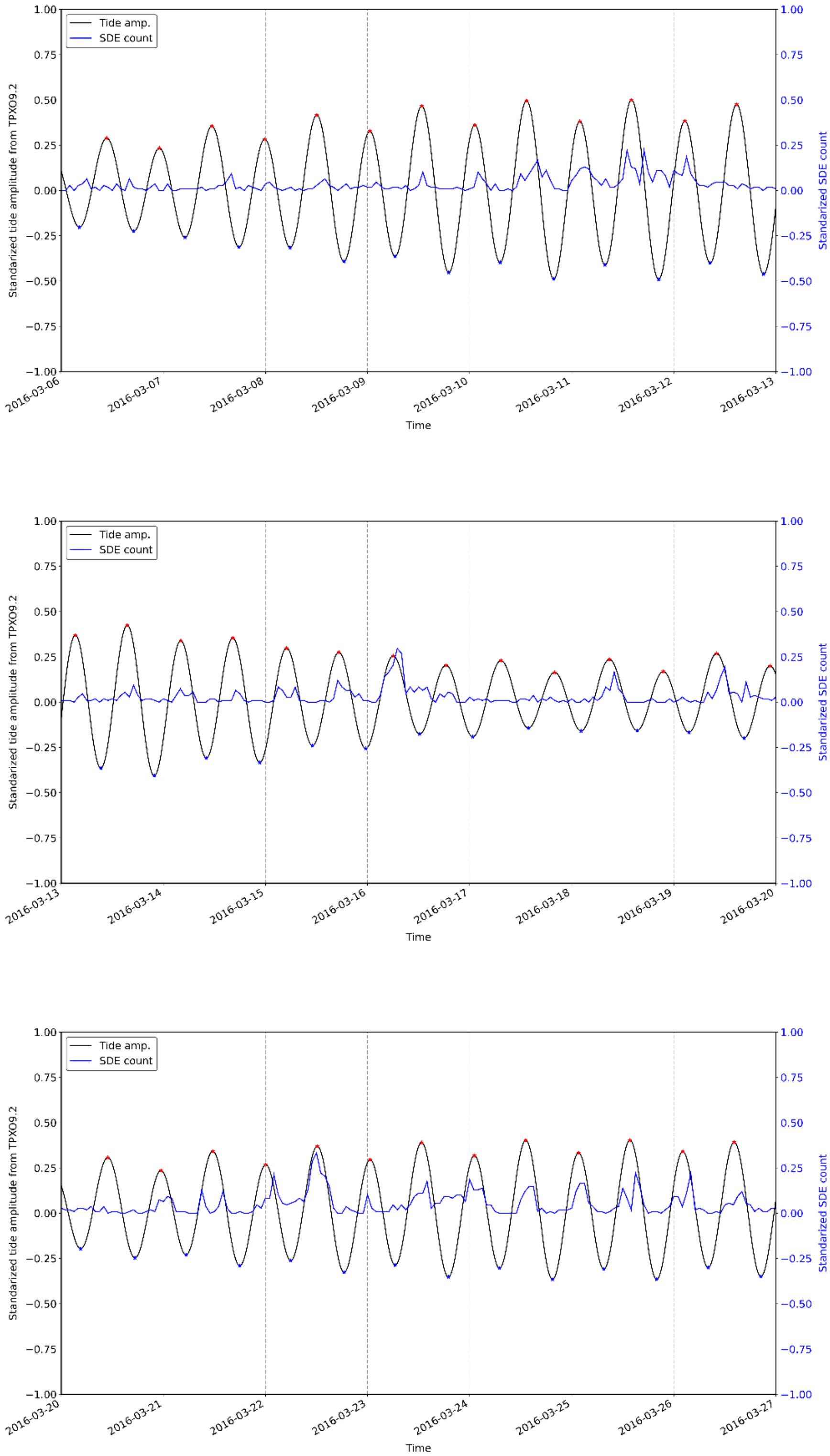

Supplementary Figure S22. Standardized plots of mean sea level amplitude change due to tides (black line) superimposed on short duration events hourly count on OBS-4 (blue line) for weeks 22-24 of survey (6.3-27.3.2016).

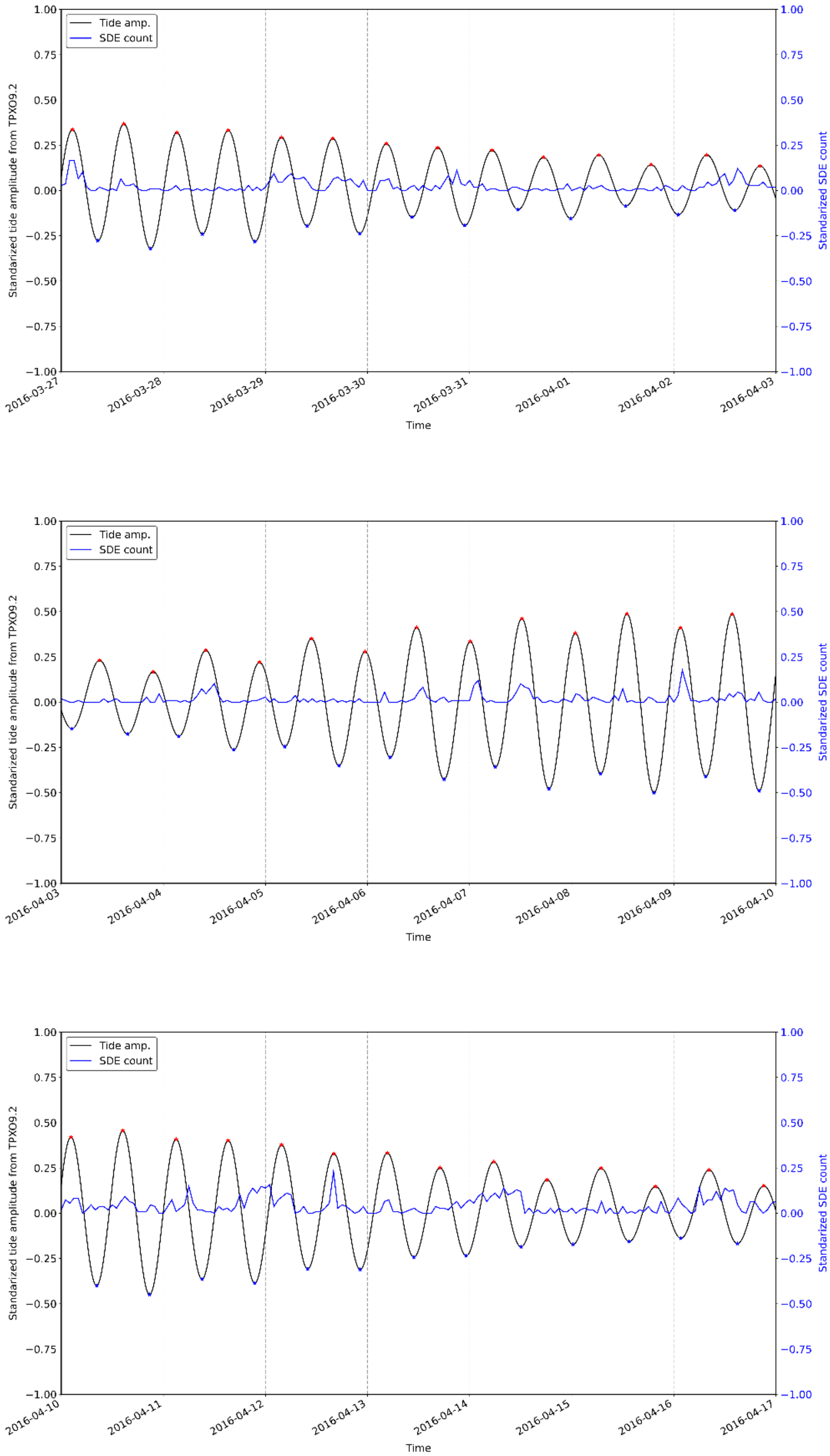

Supplementary Figure S23. Standardized plots of mean sea level amplitude change due to tides (black line) superimposed on short duration events hourly count on OBS-4 (blue line) for weeks 25-27 of survey (27.3-17.4.2016).

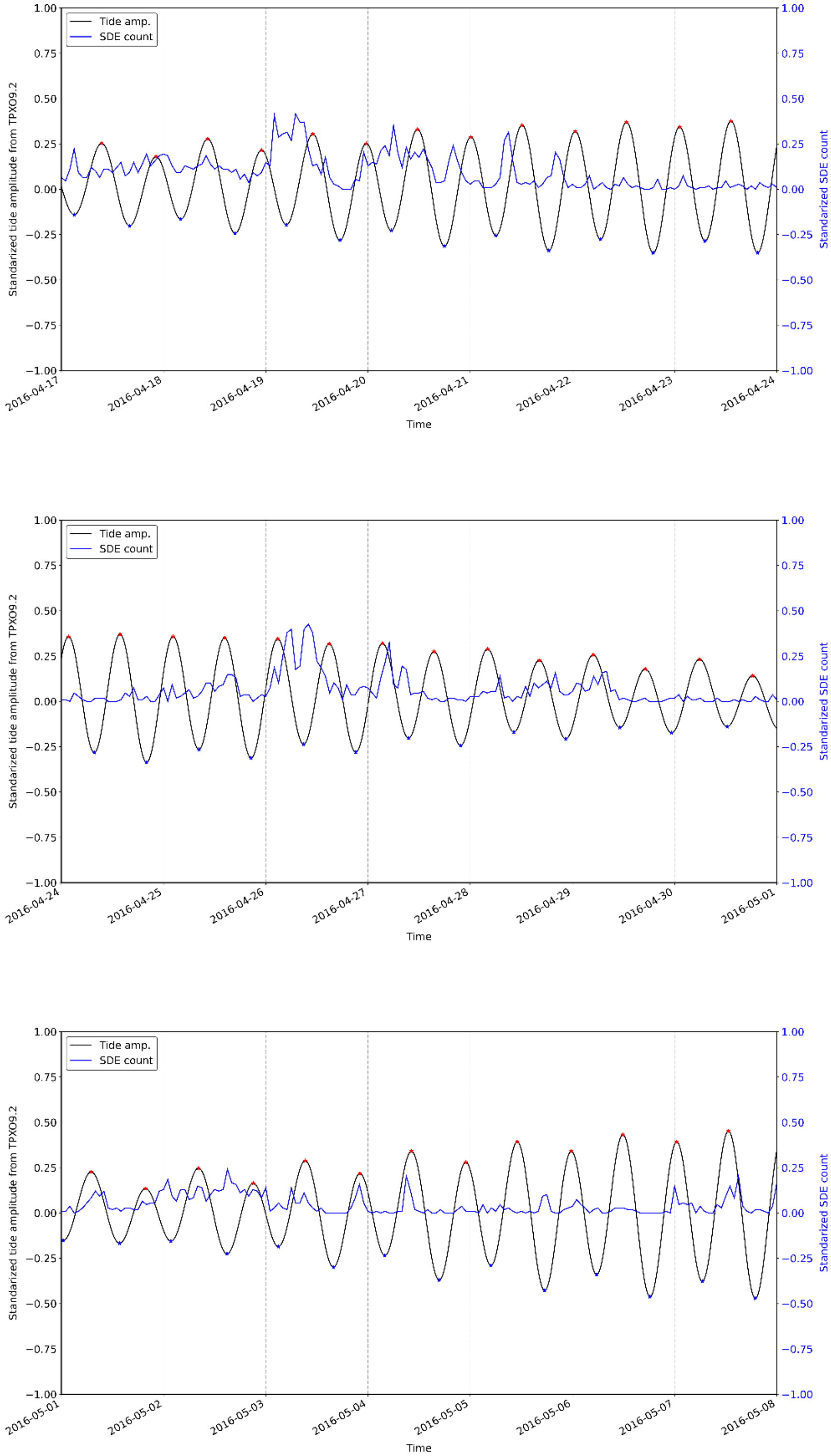

Supplementary Figure S24. Standardized plots of mean sea level amplitude change due to tides (black line) superimposed on short duration events hourly count on OBS-4 (blue line) for weeks 28-30 of survey (17.4-8.5.2016).

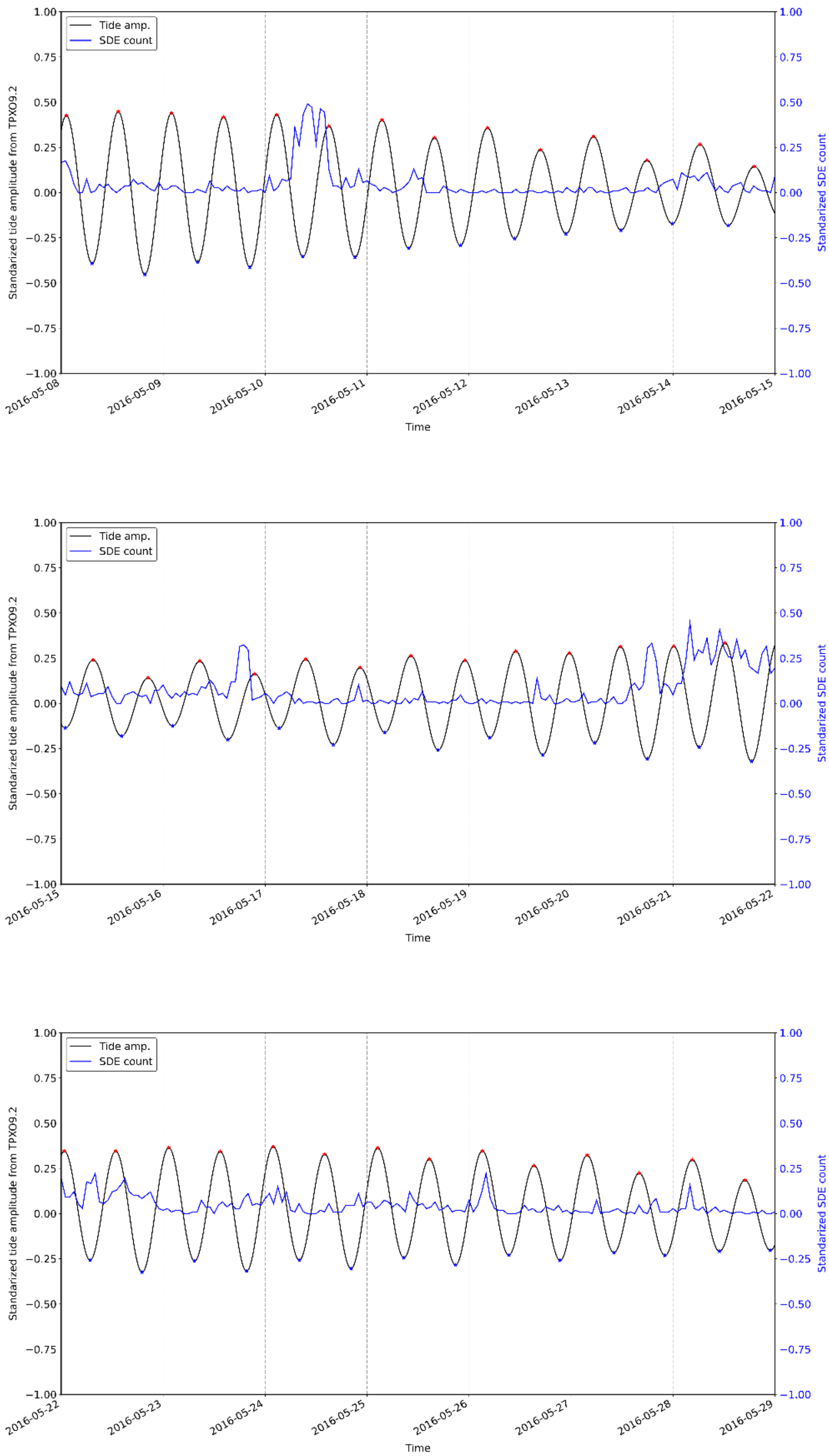

Supplementary Figure S25. Standardized plots of mean sea level amplitude change due to tides (black line) superimposed on short duration events hourly count on OBS-4 (blue line) for weeks 31-33 of survey (8.5-29.5.2016).

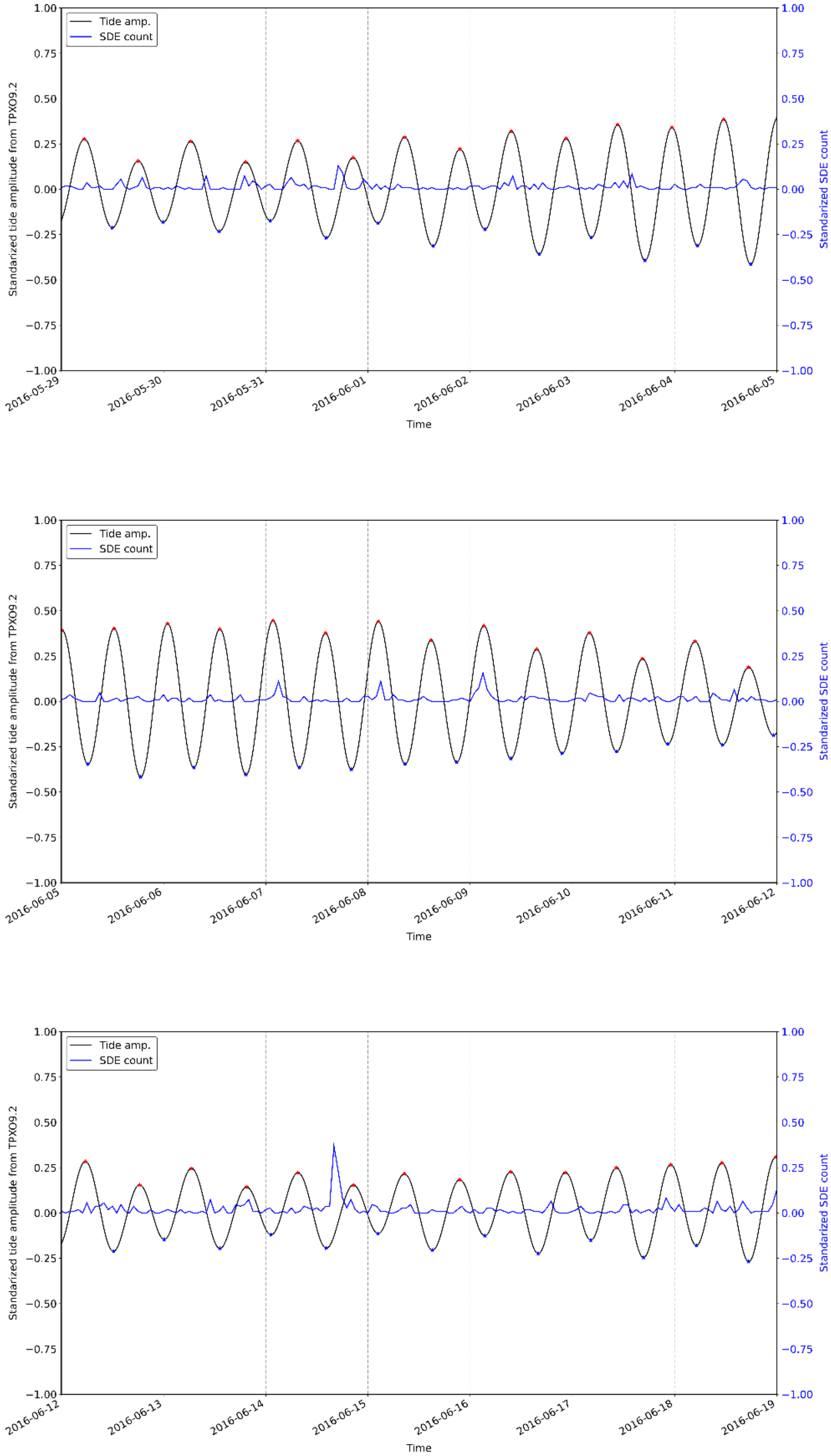

Supplementary Figure S26. Standardized plots of mean sea level amplitude change due to tides (black line) superimposed on short duration events hourly count on OBS-4 (blue line) for weeks 34-36 of survey (29.5-19.6.2016).

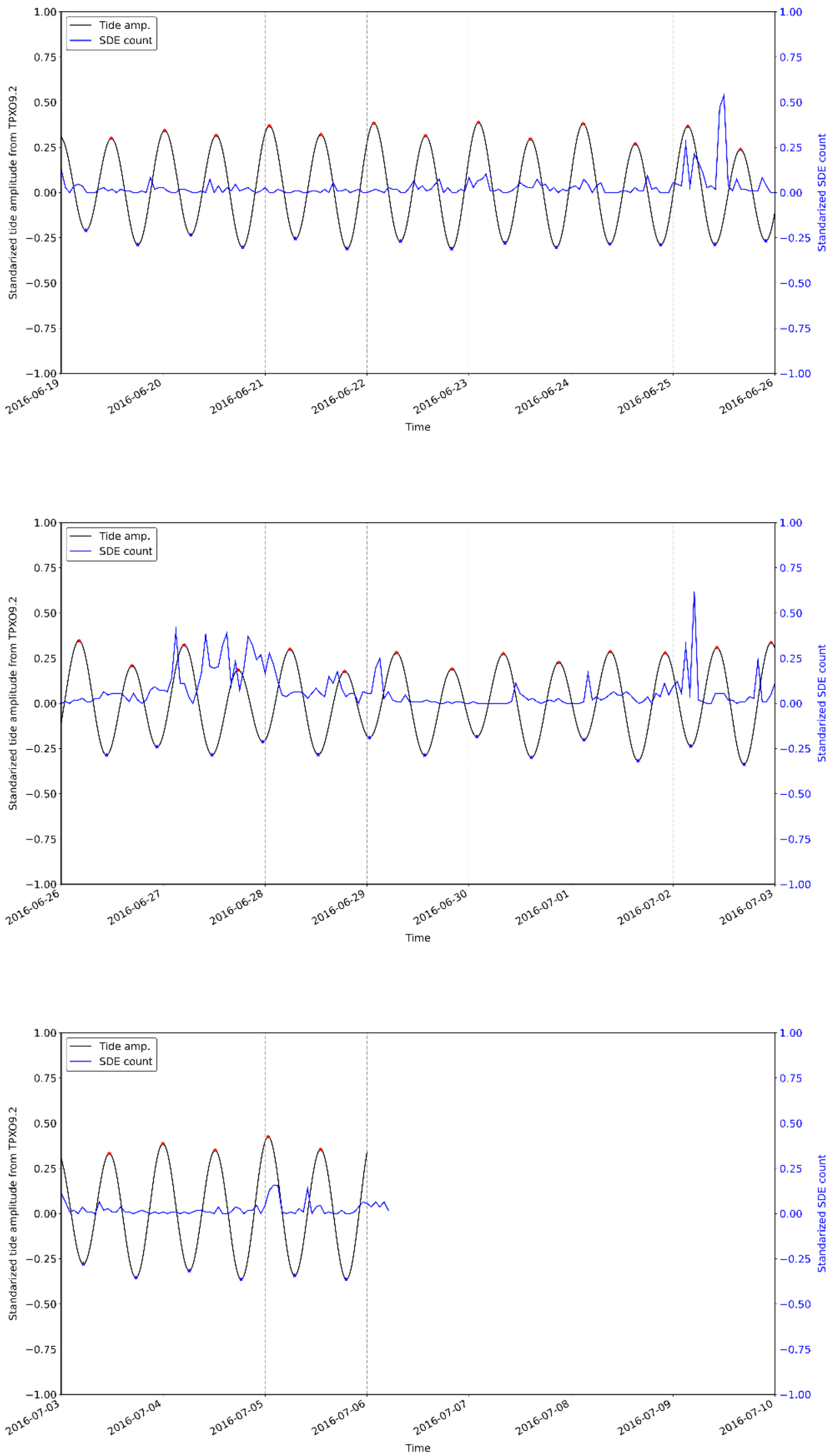

Supplementary Figure S27. Standardized plots of mean sea level amplitude change due to tides (black line) superimposed on short duration events hourly count on OBS-4 (blue line) for weeks 37-39 of survey (19.6-6.7.2016).

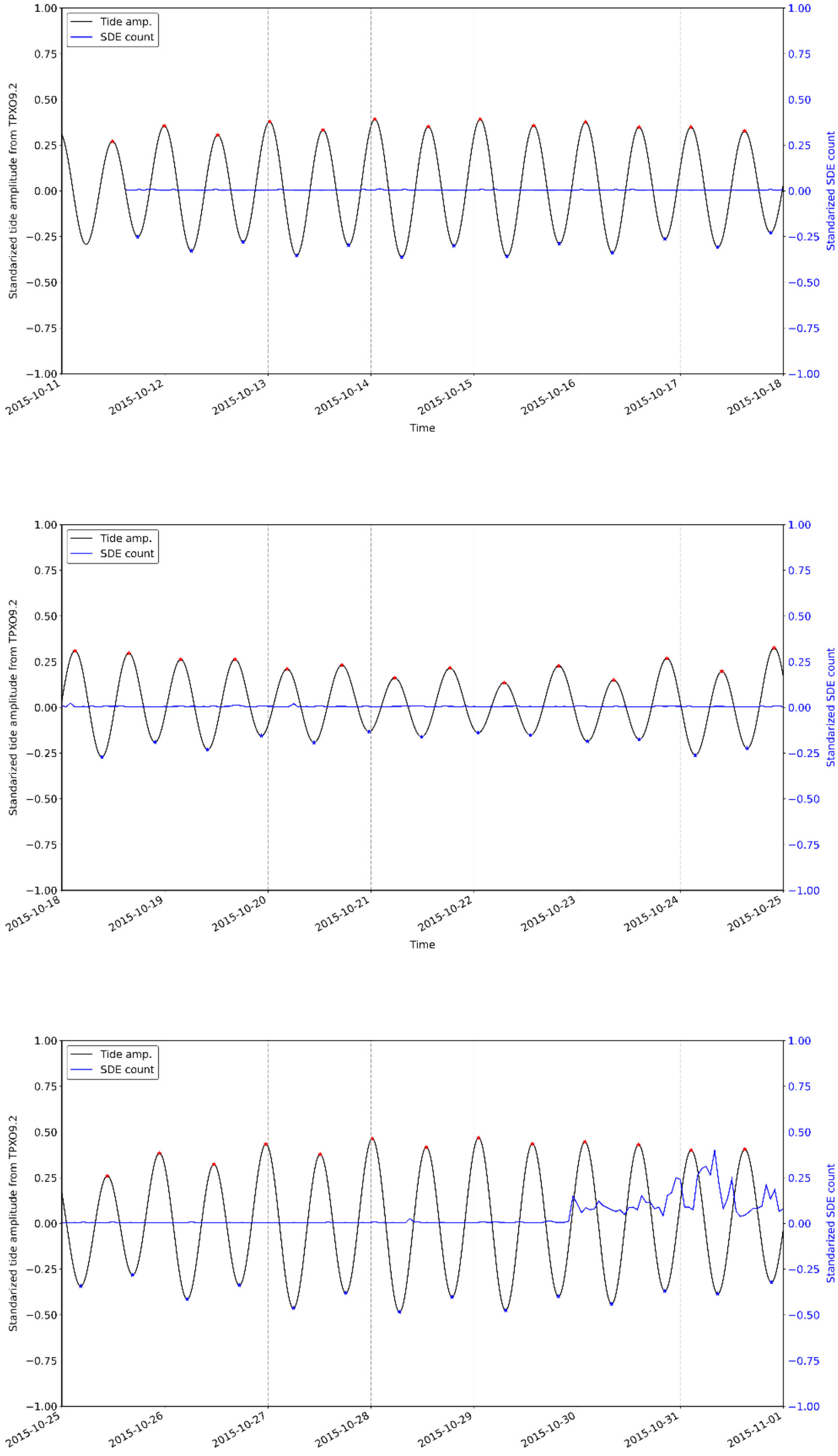

Supplementary Figure S28. Standardized plots of mean sea level amplitude change due to tides (black line) superimposed on short duration events hourly count on OBS-5 (blue line) for weeks 1-3 of survey (11.10-1.11.2015).

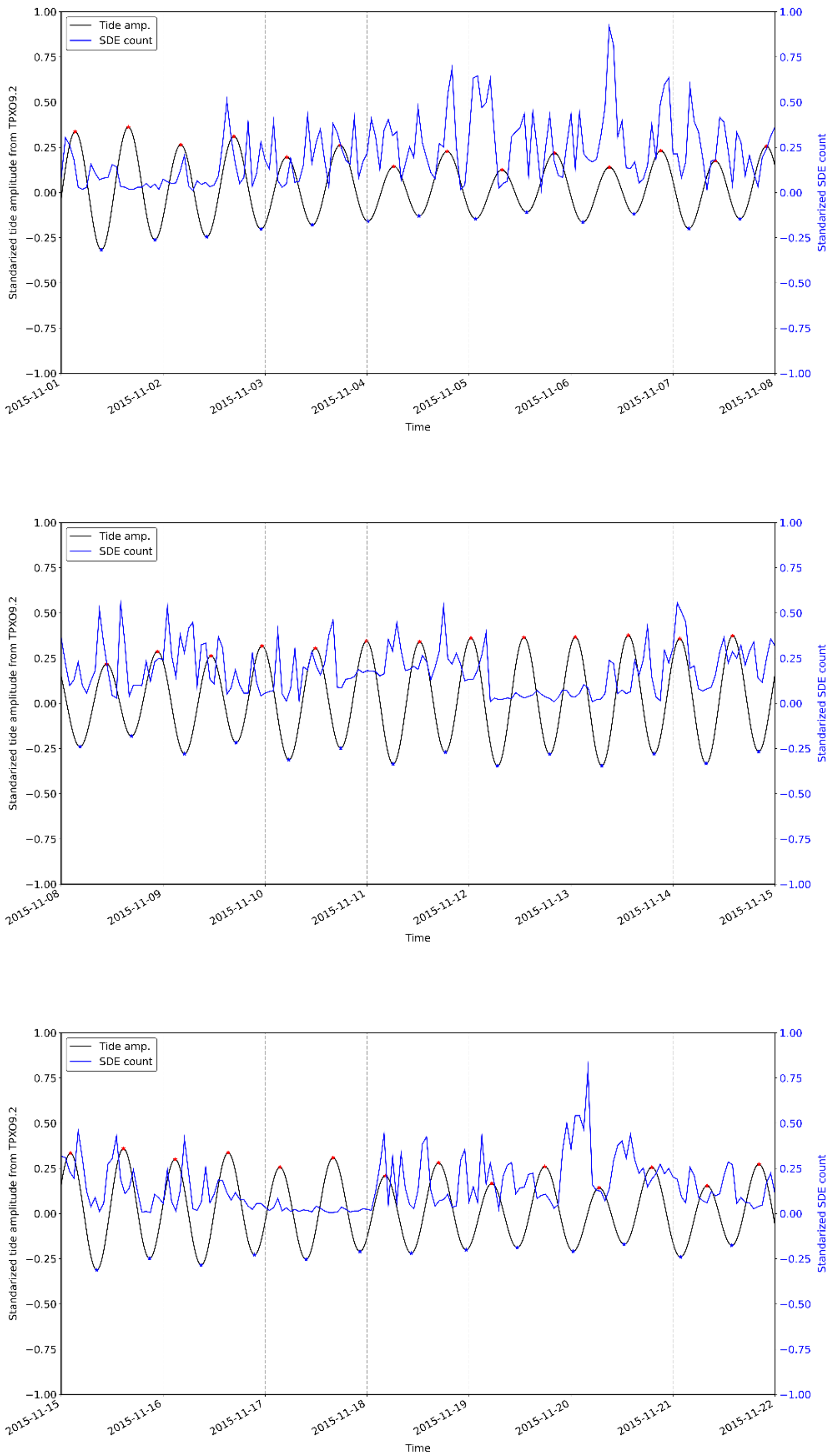

Supplementary Figure S29. Standardized plots of mean sea level amplitude change due to tides (black line) superimposed on short duration events hourly count on OBS-5 (blue line) for weeks 4-6 of survey (1.11-22.11.2015).

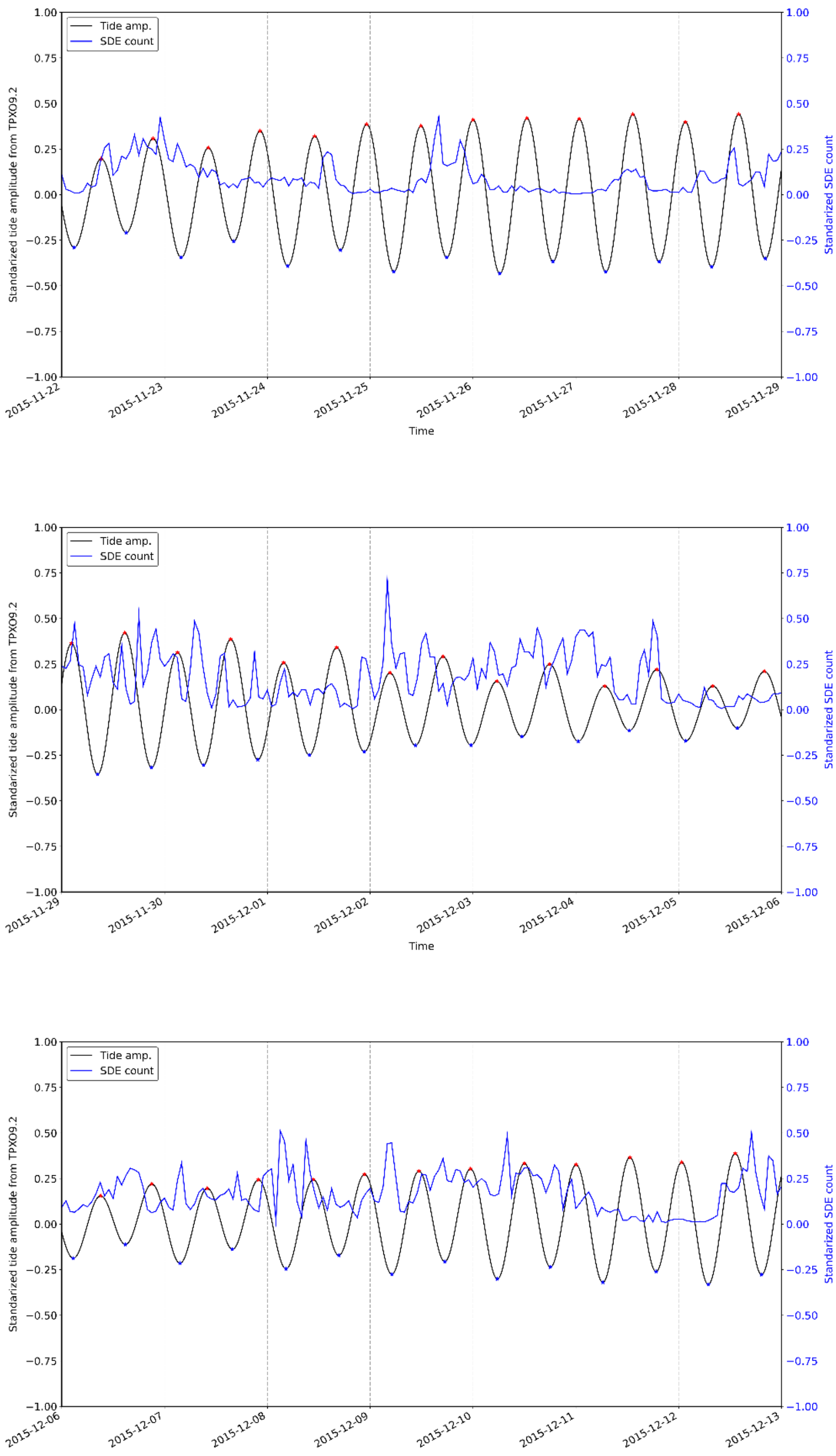

Supplementary Figure S30. Standardized plots of mean sea level amplitude change due to tides (black line) superimposed on short duration events hourly count on OBS-5 (blue line) for weeks 7-9 of survey (22.11-13.12.2015).

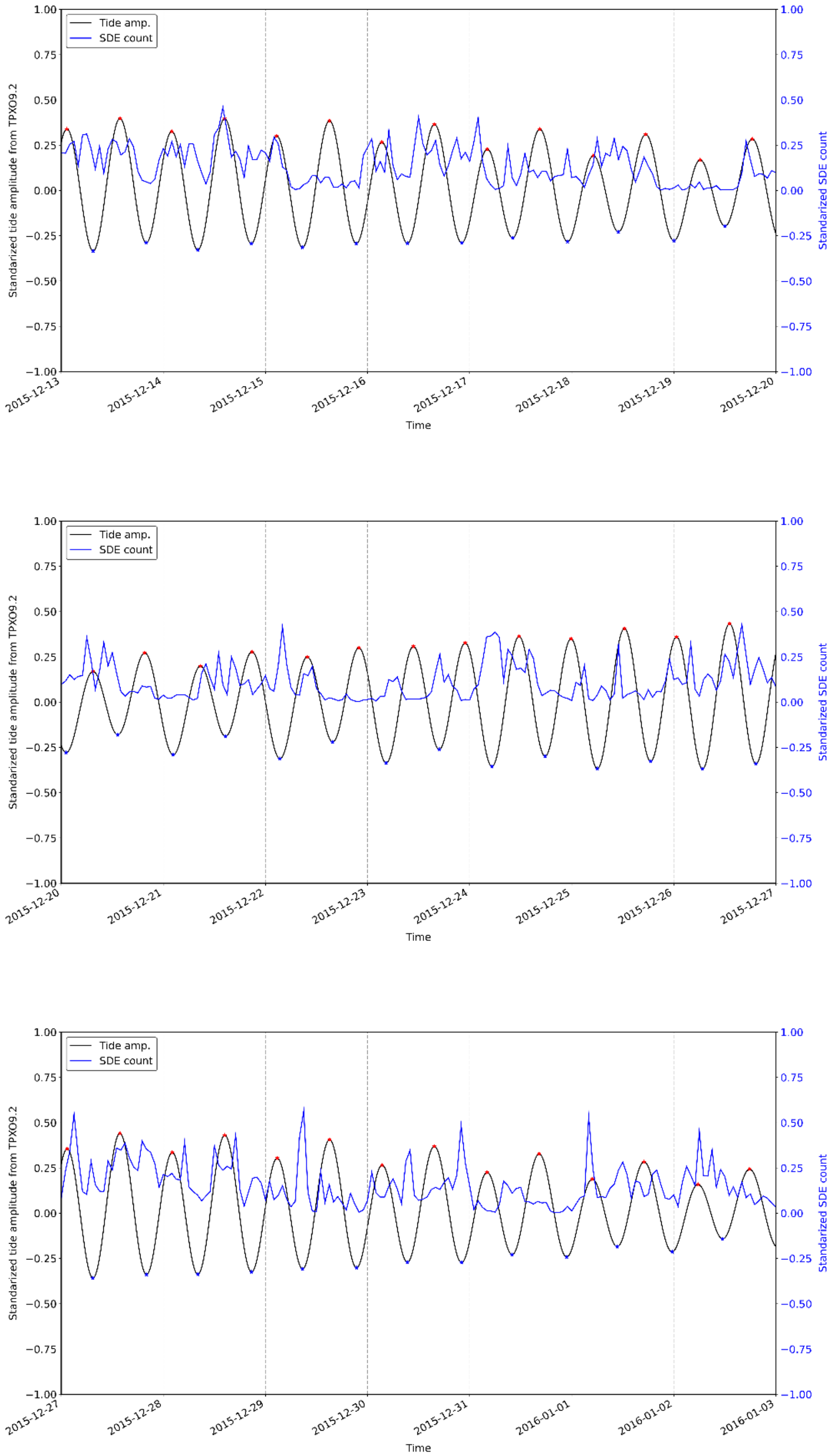

Supplementary Figure S31. Standardized plots of mean sea level amplitude change due to tides (black line) superimposed on short duration events hourly count on OBS-5 (blue line) for weeks 10-12 of survey (13.12.2015-3.1.2016).

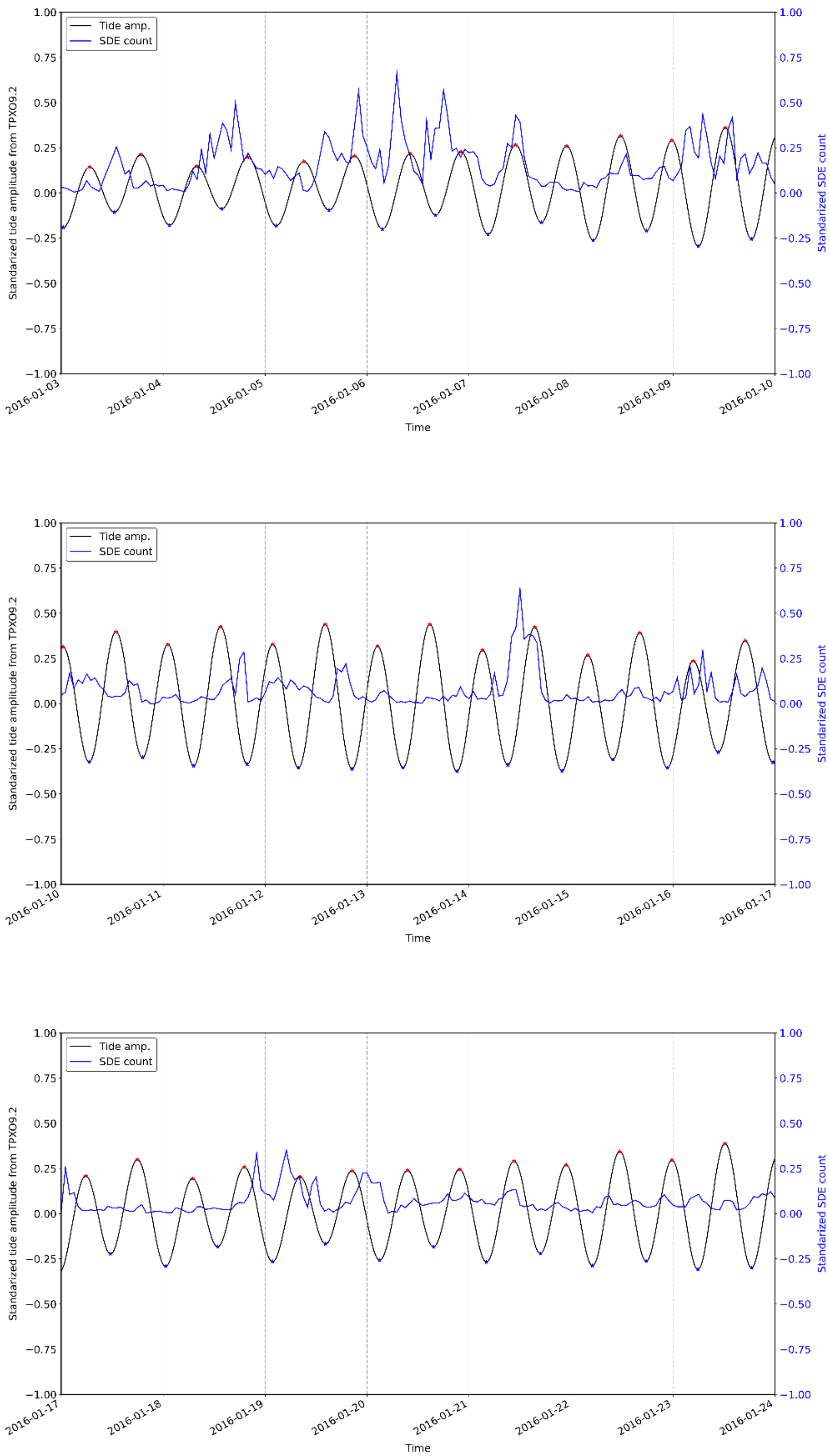

Supplementary Figure S32. Standardized plots of mean sea level amplitude change due to tides (black line) superimposed on short duration events hourly count on OBS-5 (blue line) for weeks 13-15 of survey (3.1-24.1.2016).

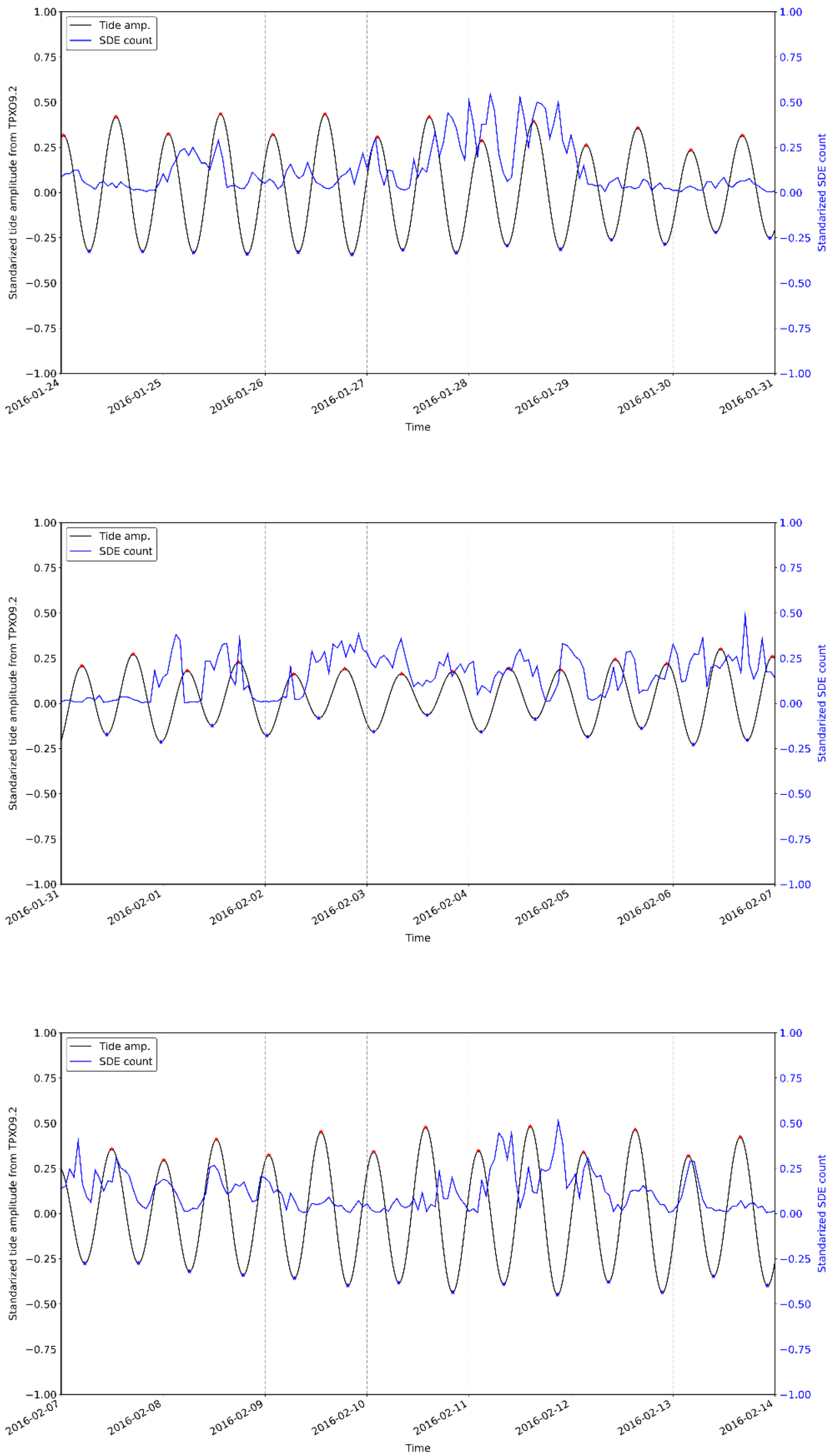

Supplementary Figure S33. Standardized plots of mean sea level amplitude change due to tides (black line) superimposed on short duration events hourly count on OBS-5 (blue line) for weeks 16-18 of survey (24.1-14.2.2016).

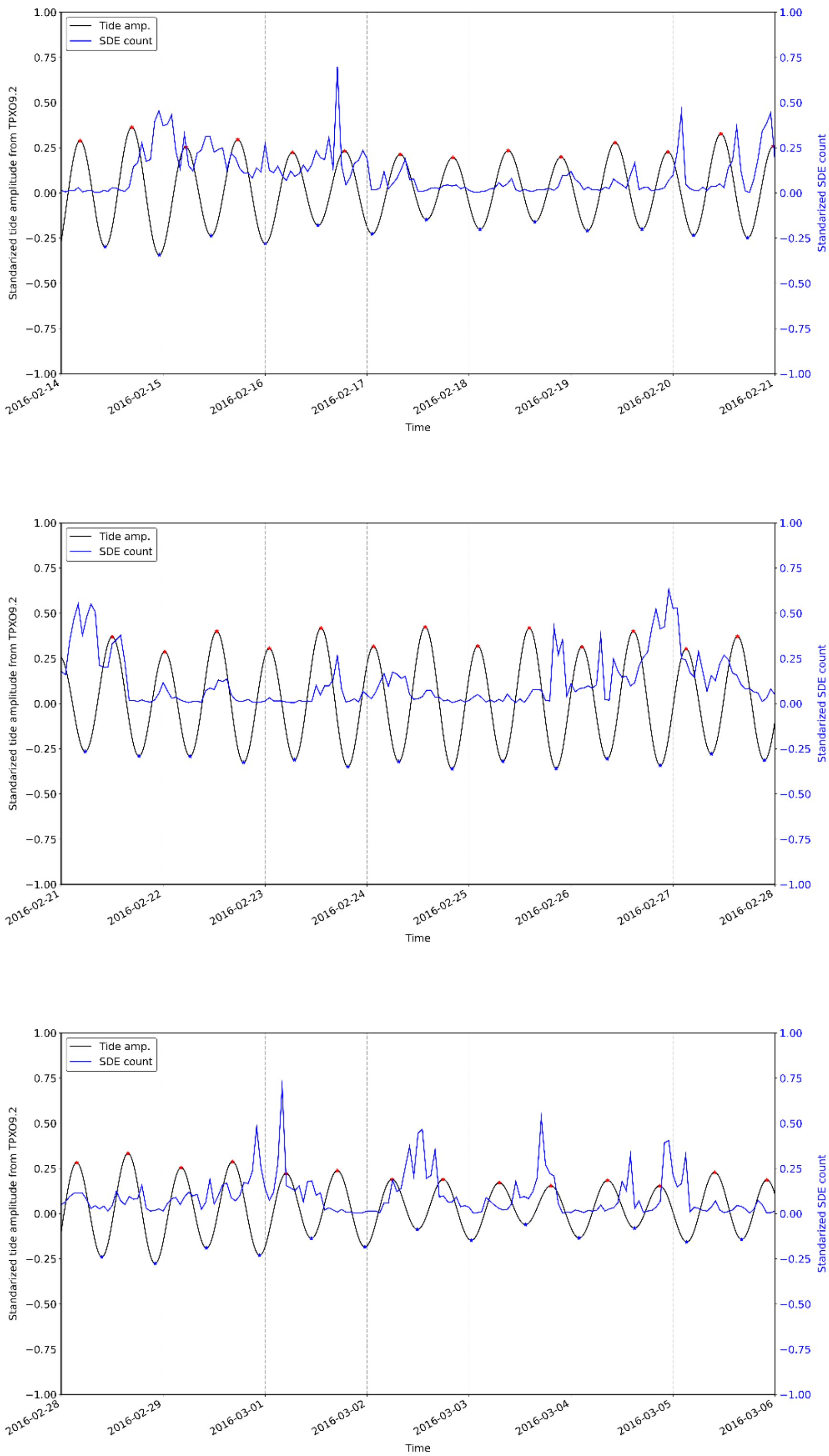

Supplementary Figure S34. Standardized plots of mean sea level amplitude change due to tides (black line) superimposed on short duration events hourly count on OBS-5 (blue line) for weeks 19-21 of survey (14.2-6.3.2016).

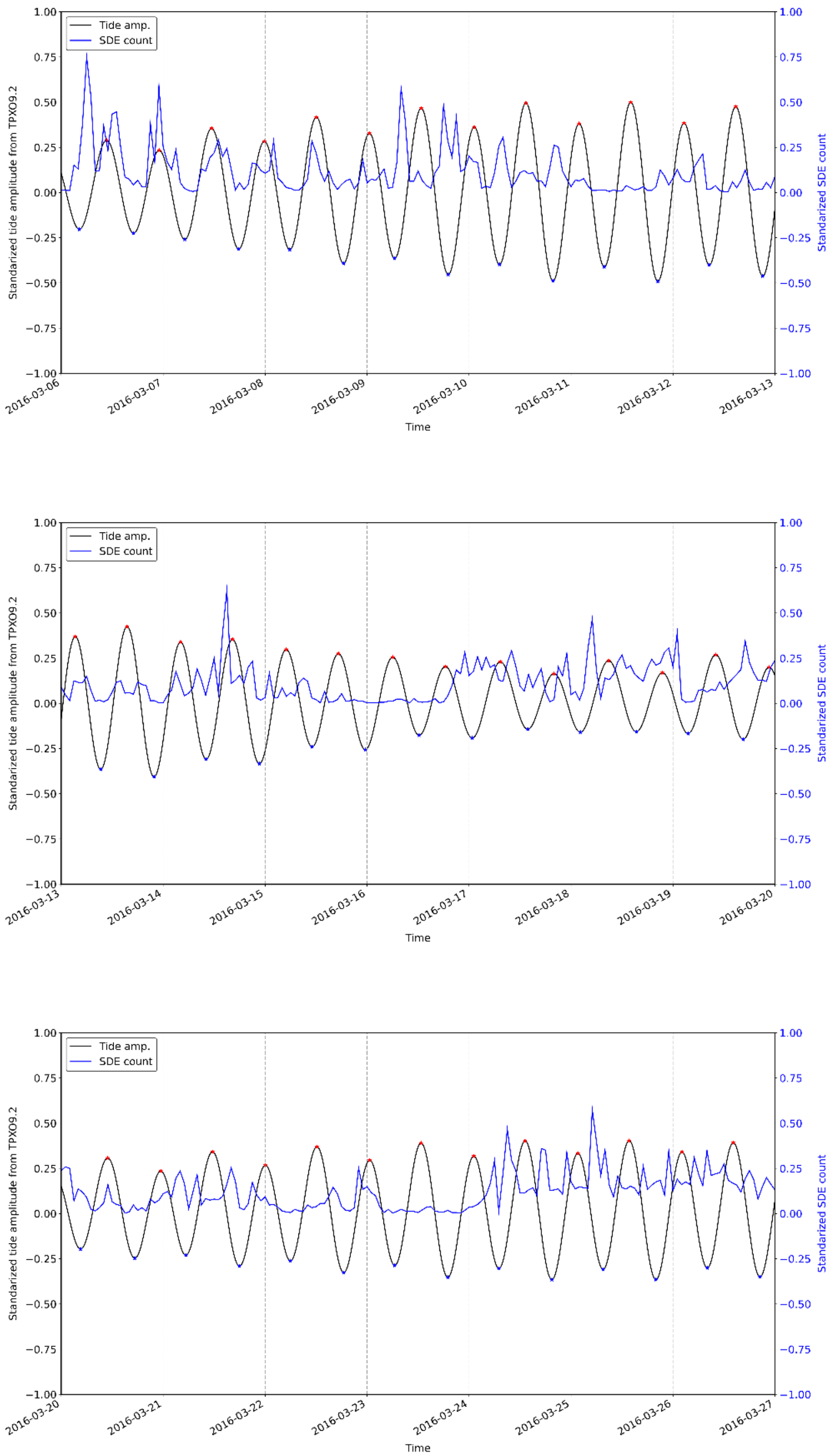

Supplementary Figure S35. Standardized plots of mean sea level amplitude change due to tides (black line) superimposed on short duration events hourly count on OBS-5 (blue line) for weeks 22-24 of survey (6.3-27.3.2016).

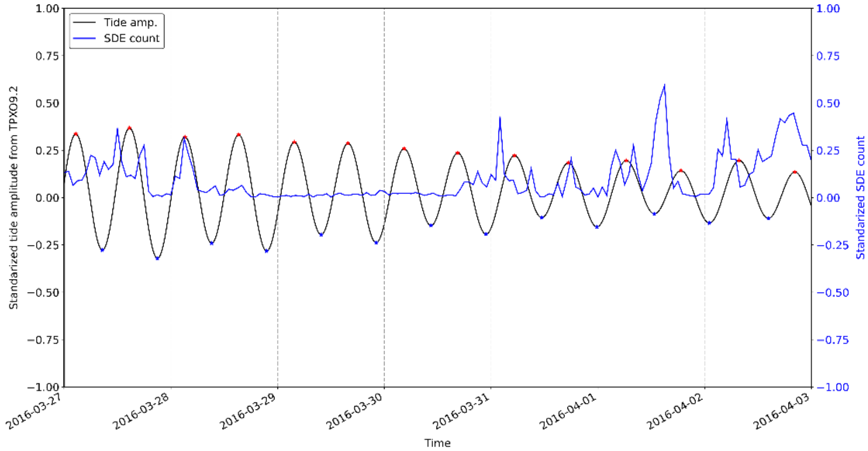

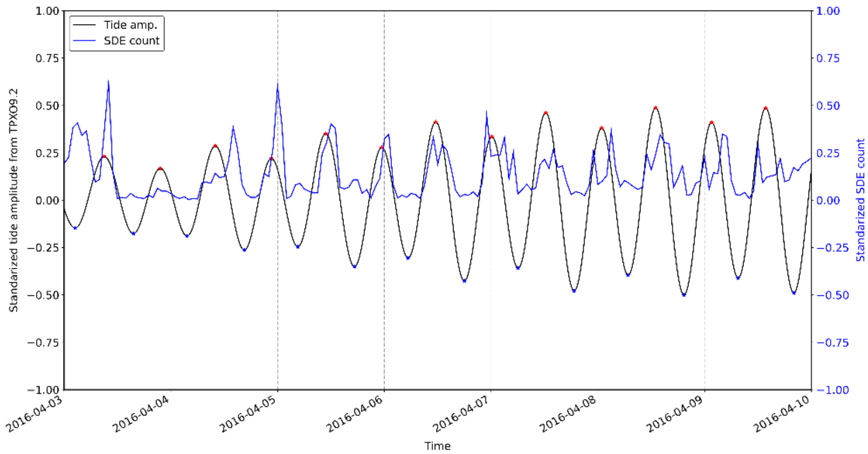

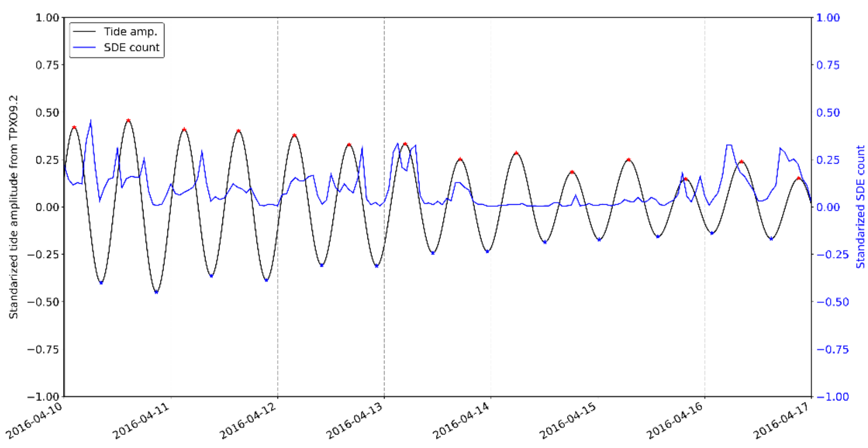

Supplementary Figure S36. Standardized plots of mean sea level amplitude change due to tides (black line) superimposed on short duration events hourly count on OBS-5 (blue line) for weeks 25-27 of survey (27.3-17.4.2016).

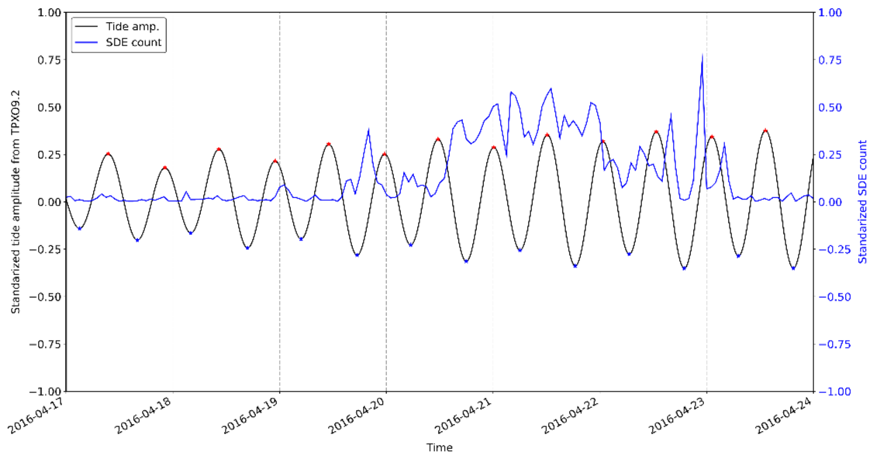

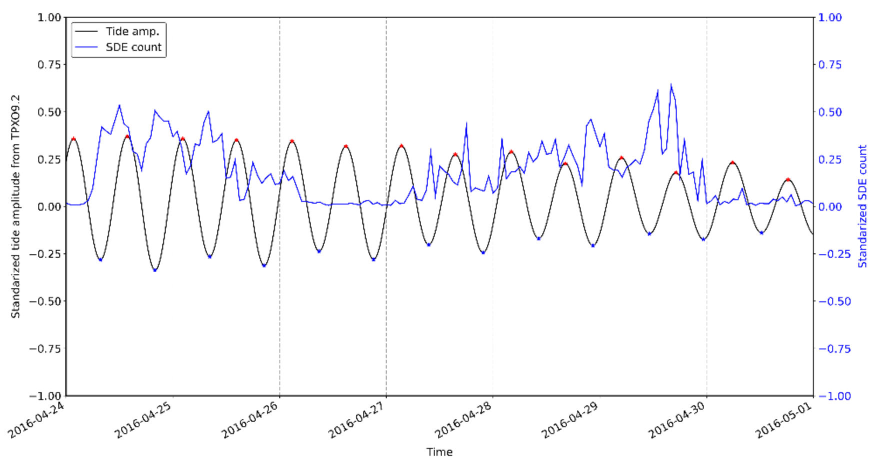

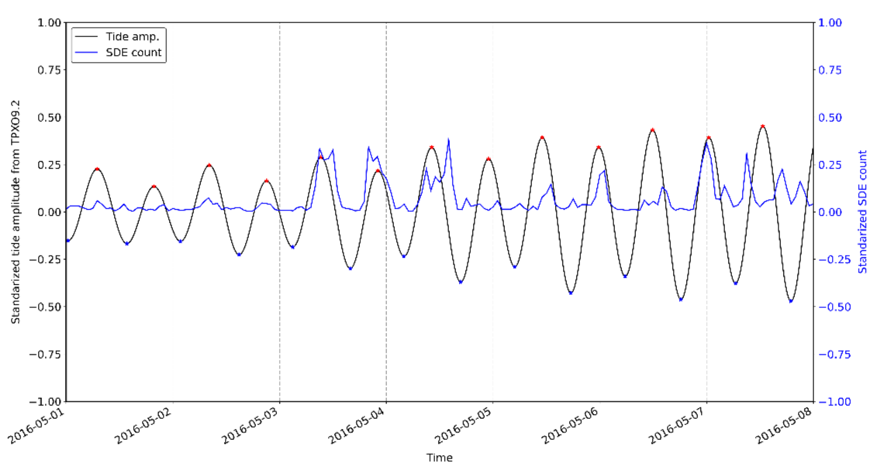

Supplementary Figure S37. Standardized plots of mean sea level amplitude change due to tides (black line) superimposed on short duration events hourly count on OBS-5 (blue line) for weeks 28-30 of survey (17.4-8.5.2016).

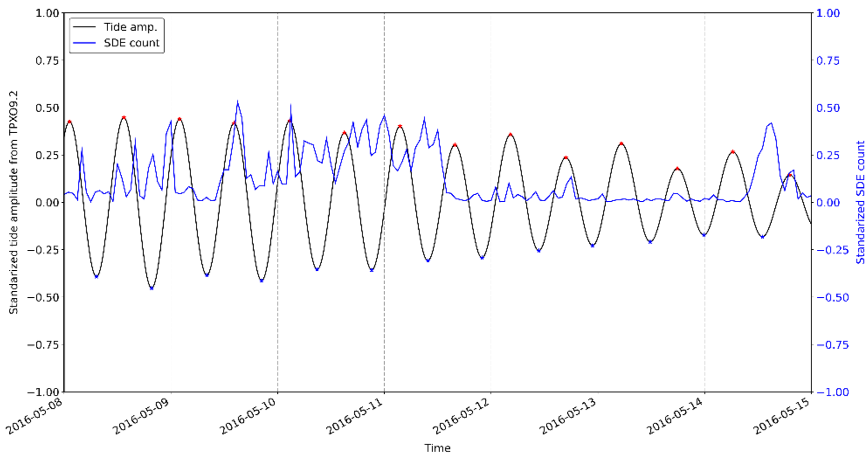

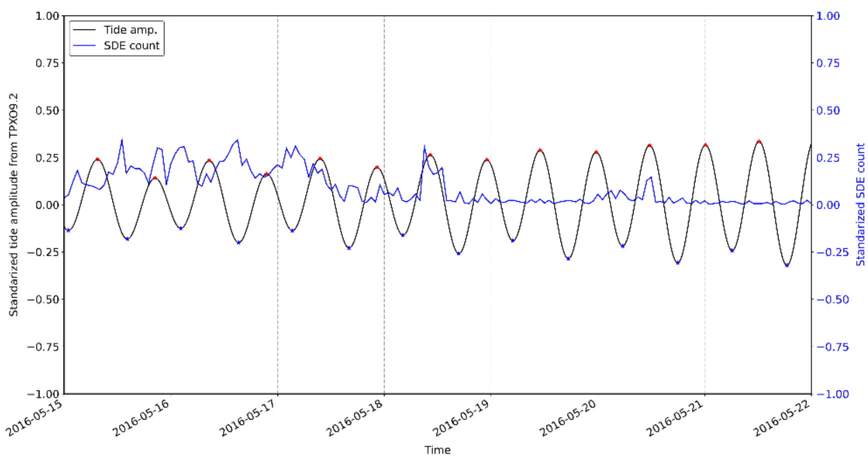

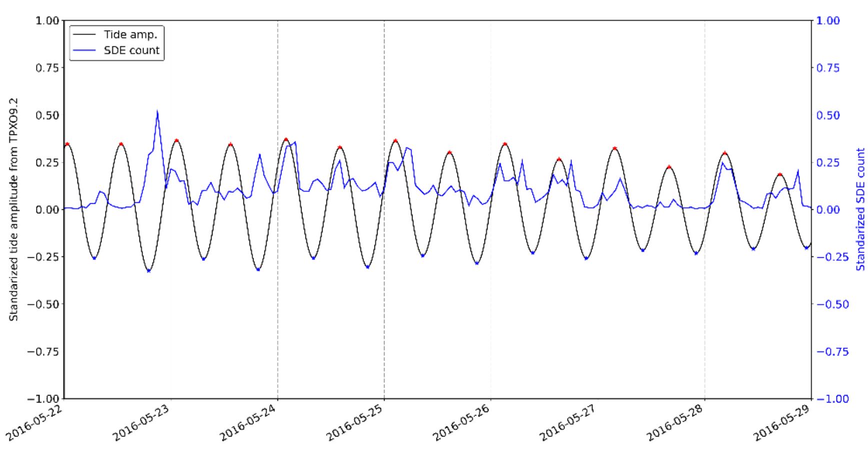

Supplementary Figure S38. Standardized plots of mean sea level amplitude change due to tides (black line) superimposed on short duration events hourly count on OBS-5 (blue line) for weeks 31-33 of survey (8.5-29.5.2016).

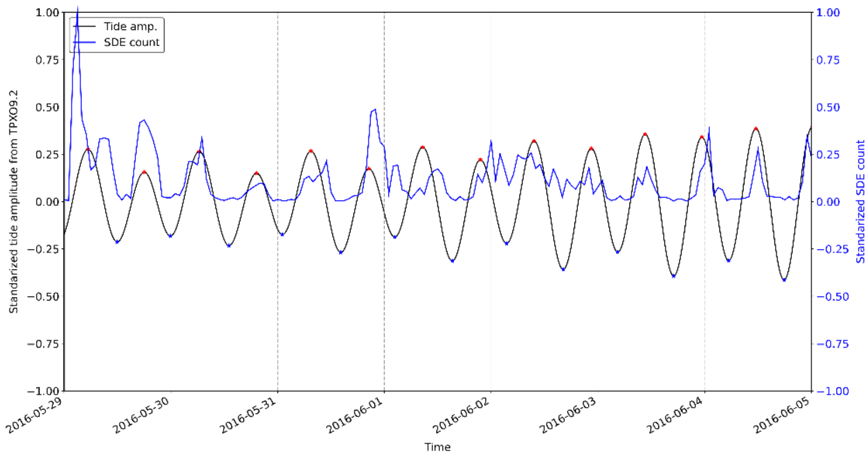

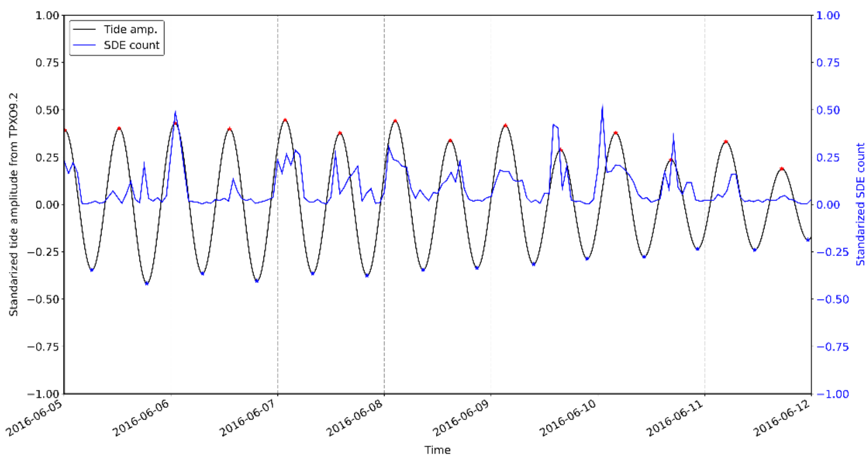

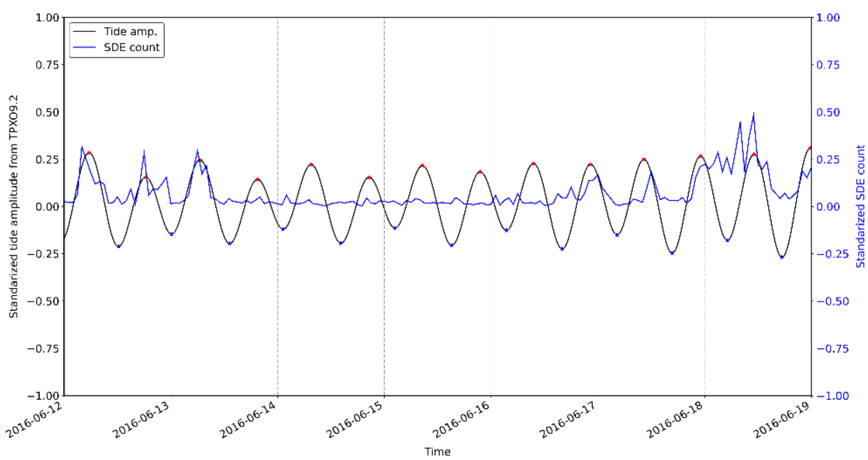

Supplementary Figure S39. Standardized plots of mean sea level amplitude change due to tides (black line) superimposed on short duration events hourly count on OBS-5 (blue line) for weeks 34-36 of survey (29.5-19.6.2016).

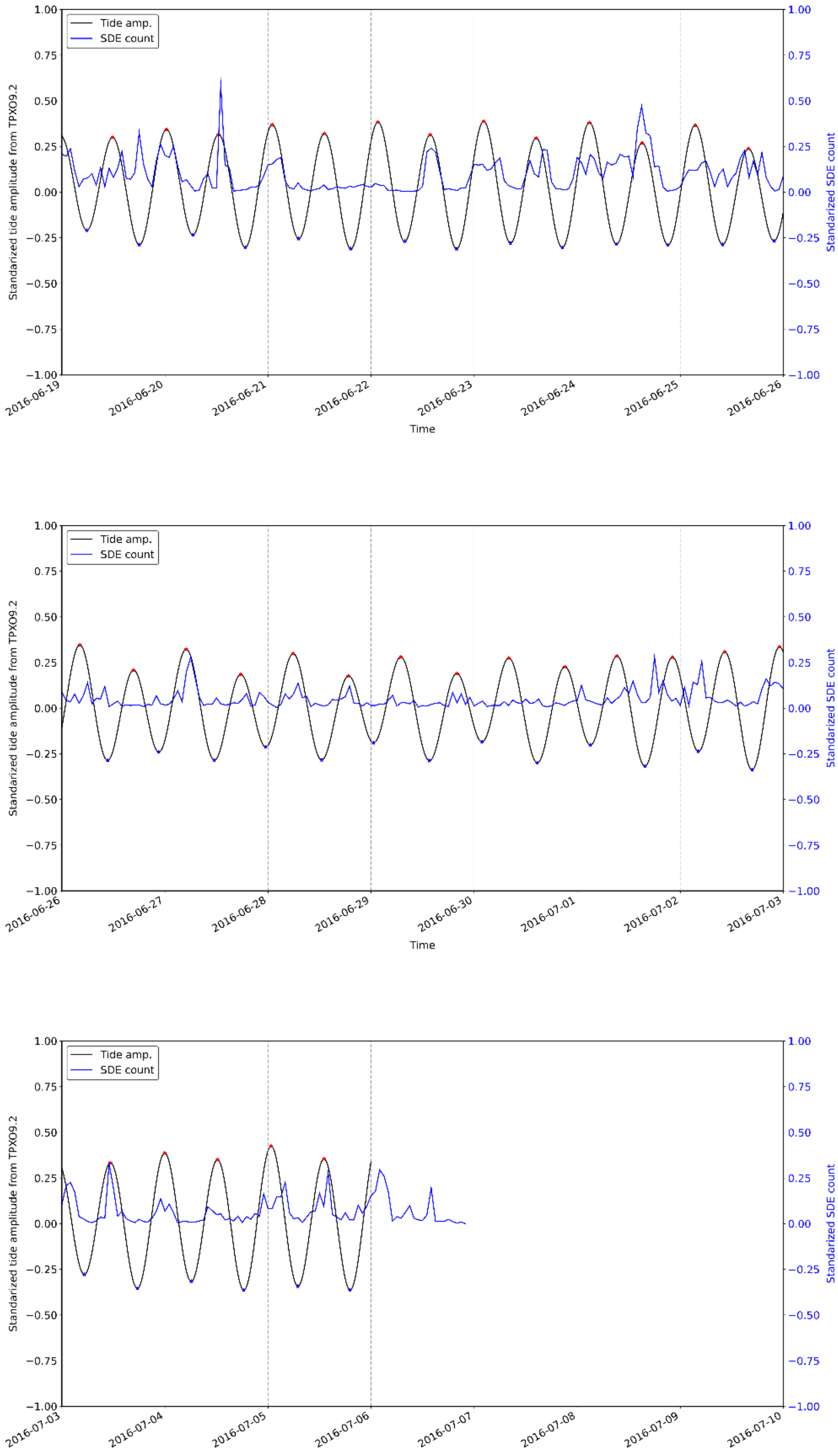

Supplementary Figure S40. Standardized plots of mean sea level amplitude change due to tides (black line) superimposed on short duration events hourly count on OBS-5 (blue line) for weeks 37-39 of survey (19.6-7.7.2016).

3.2 Supplementary Table

Symbol	Constituent	Period [hr]
M2	Principal lunar semidiurnal	12.42
M4	Shallow water overtides of principal lunar	6.21
K1	Lunar diurnal	23.93
K2	Lunisolar semidiurnal	11.97
MS4	Shallow water quarter diurnal	6.10

Supplementary Table S1. Observed tidal constituents and their corresponding periods.

4 References

Noll, M. (1969), Pitch determination of human speech by the harmonic product spectrum, the harmonic sum spectrum, and a maximum likelihood estimate, in Proceedings of the Symposium on Computer Processing in Communications, pp. 779 – 797, Polytechnic Inst. of Brooklyn, New York.

Ramakrushana Reddy, T., Dewangan, P., Arya, L., Singha, P., & Kamesh Raju, K. A. (2020). Tidal Triggering of the Harmonic Noise in Ocean-Bottom Seismometers. *Seismological Research Letters, 91*(2A), 803-813.

Roman, D. C. (2017). Automated detection and characterization of harmonic tremor in continuous seismic data. *Geophysical Research Letters, 44*(12), 6065-6073.